9-15-2011

Verification of Global Assimilation of Ionospheric Measurements Gauss Markov (GAIM-GM) Model Forecast Accuracy

Paul H. Domm

VERIFICATION OF GLOBAL ASSIMILATION OF IONOSPHERIC MEASUREMENTS GAUSS MARKOV (GAIM-GM) MODEL FORECAST ACCURACY

THESIS

Paul H. Domm, 1st Lieutenant, USAF
AFIT/GAP/ENP/11-S01

DEPARTMENT OF THE AIR FORCE
AIR UNIVERSITY

AIR FORCE INSTITUTE OF TECHNOLOGY

Wright-Patterson Air Force Base, Ohio

AFIT/GAP/ENP/11-S01

VERIFICATION OF GLOBAL ASSIMILATION OF IONOSPHERIC MEASUREMENTS GAUSS MARKOV (GAIM-GM) MODEL FORECAST ACCURACY

THESIS

Presented to the Faculty

Department of Engineering Physics

Graduate School of Engineering and Management

Air Force Institute of Technology

Air University

Air Education and Training Command

In Partial Fulfillment of the Requirements for the

Degree of Master of Science

Paul H. Domm, BS
1st Lieutenant, USAF

September 2011

AFIT/GAP/ENP/11-S01

VERIFICATION OF GLOBAL ASSIMILATION OF IONOSPHERIC MEASUREMENTS GAUSS MARKOV (GAIM-GM) MODEL FORECAST ACCURACY

Paul H. Domm, BS
1st Lieutenant, USAF

Approved:

//signed//	7 Sept 2011
Lt Col Robb M. Randall (Chairman)	Date
//signed//	7 Sept 2011
Lt Col Ariel O. Acebal (Member)	Date
//signed//	7 Sept 2011
Larry C. Gardner, PhD (Member)	Date

Abstract

GAIM-GM is an operational Kalman filter data assimilation model of the ionosphere that can assimilate data from GPS total electron content (TEC), ionosonde electron density profiles, and satellite-based in-situ electron densities. The Air Force Weather Agency (AFWA) uses GAIM-GM to specify and forecast the ionosphere, however, an in-depth investigation into the accuracy of these forecasts has not been completed. GAIM-GM output obtained from four cases run from combinations of geomagnetic and solar activity was used to determine GAIM-GM forecast accuracy. Forecast accuracy was determined through the use of a skill score as well as other statistical tools to include root mean square error (RMSE) and percent differences between the forecasts and the observations. It is determined that overall, GAIM-GM forecast output is more representative than the climatological reference 90% of the time indicating that GAIM-GM can therefore forecast short term fluctuations in the ionosphere. Skill scores decrease at night and GAIM-GM shows an overall diurnal bias to under forecast at night and over forecast during the day. The RMSE increases during daytime, geomagnetic storming and during solar maximum.

Acknowledgements

I must first thank Lt Col Robb Randall, my thesis advisor, for his willingness to take me on as a student at the end of his time at AFIT. I would not have succeeded had it not been for his expertise, good humor, encouragement and direction in carrying out this research. I am grateful for his effort, especially behind the scenes, on my behalf to ensure that the work progressed.

I would also like to thank Lt Col Ariel Acebal, a member of my thesis committee, for his help and suggestions for all things space weather related. I am grateful for his time spent getting sufficiently confused with me and Lt Col Randall as we talked through the problems of the day. Without his insight, the confusion may have never left.

To the good folks at Utah State University, to include Drs. Robert Schunk, Ludger Scherliess and my final thesis committee member, Dr. Larry Gardner, may I say thank you. Their timely assistance and insight into the research was more than I could have hoped for.

Finally, I need to thank my wife and kids for giving me daily reminders of what is truly important in life. Their prayers and encouragement are what kept me afloat when I felt like I was sinking. The successful completion of this thesis was powered by their love.

Paul H. Domm

Table of Contents

Page

List of Figures

List of Tables

VERIFICATION OF GLOBAL ASSIMILATION OF IONOSPHERIC MEASUREMENTS GAUSS MARKOV (GAIM-GM) MODEL FORECAST ACCURACY

I. Introduction

1.1 Motivation and Background

Since the dawn of the space age, technological advances such as long range communication, Global Positioning System (GPS) navigation and space based surveillance have advanced at a torrid pace and continue to do so. These space based capabilities are routinely used and exploited in both military and civilian operations. Our collective dependence on these capabilities is unquestioned, thus, it is imperative to fully understand how the space environment behaves, since it impacts these systems.

The ionosphere is the near earth subset of the space environment that is located roughly between 90 km-1500 km above the earth. Satellite, navigation and communication based capabilities operate in this dynamic environment. It is critical, therefore, to fully understand and accurately model the ionosphere in order to mitigate potential threats to these space based capabilities. These threats include, but are not limited to, radio communication blackouts and navigational errors associated with fluctuations in the ionosphere.

Ionospheric and space weather models are improving, owing in part, to the increase in available ionospheric data from GPS satellites, military satellites and land based ionospheric readings. The improvement in space weather and ionospheric models gives military and civilian decision makers greater tools and confidence in predicting the behavior of the ionosphere and therefore greater ability to plan and make decisions critical to military operations and national security.

The Global Assimilation of Ionospheric Measurements Gauss-Markov model developed at Utah State University and currently operational at the Air Force Weather Agency is a physics based data assimilation model of the ionosphere that generates both specifications (nowcasts) and forecasts of the ionosphere. Validation studies have been conducted to determine the accuracy of the specifications, but little work has been focused on verifying forecast accuracy.

1.2 Research objectives

This work aims to determine the forecast accuracy of GAIM-GM as run by AFWA. The end goal is to determine the accuracy, strengths and weaknesses of the model. This information will aid the developers, operators and end users of GAIM-GM to improve upon and better understand the limitations of the model. This is done by running GAIM-GM for several cases that include variations in geomagnetic and solar activity as well as focusing over both the entire globe and CONUS. The forecasts and a climatological reference background are compared to the ionospheric specification to determine the forecast accuracy with respect to climatology via a forecast skill score. Forecast accuracy is evaluated through statistical tools to include root mean square error (RMSE) and percent differences between the forecasts and the specifications.

1.3 Document Structure

There are 5 chapters in this work. Chapter I is an introduction. Chapter II provides background information about GAIM-GM, the Ionospheric Forecast Model (IFM), the data used in the research, the Kalman filter, and the statistical tools used to determine forecast accuracy to include the forecast skill score. Chapter III focuses on the methodology in executing the forecast accuracy verification. Such items include, the geophysical conditions of each case, how GAIM-GM is run, what data is used, how the skill scores are determined and pertinent assumptions to ensure the model is operated similarly to how it is operated at AFWA. Chapter IV contains the results and analysis of the verification findings and Chapter V provides a summary of the work as well as conclusions and suggestions for continuing work on this topic.

II. Background

This chapter lays the groundwork for the remainder of the paper. It begins by describing the ionosphere and then moves on to introducing GAIM-GM and its input model, the IFM. Sections on the data ingested into GAIM-GM, the Kalman filter and skill scores are included. Finally, previous validation research is summarized to justify the assumptions for the methodology used in performing the forecast accuracy verification.

2.1 The Ionosphere and Plasmasphere

The ionosphere is located from 60 km to more than 1000 km above Earth and is so named due to the presence of ions within this region. Neutral molecules are ionized from extreme ultraviolet (EUV) and Soft X-ray radiation from the sun in a process called photoionization. These ions are then subject to the processes of chemical reactions, diffusion, recombination, and transport by the neutral winds. Variations in latitude, the day-night sector, the Earth's magnetic field and the previously mentioned processes create various regions within the ionosphere denoted the D, E, F regions and the topside ionosphere, illustrated in Figure 1 (*Schunk and Nagy*, 2009).

The D region is found between 60 km-100 km and is heavily influenced by complex chemical reactions. The E region is located between 100 km–150 km and is likewise dominated by chemical processes, albeit less than the D region, and is characterized as a weakly ionized plasma (*Schunk and Nagy*, 2009).

The partially ionized F region is broken up into two components, the F_1 and F_2 layers located between 150 km-250 km and around 300 km respectively. Ion transport processes begin to dominate over chemical processes in this region and the point where

chemical and transport processes balance is denoted the F_2 peak as ion densities reach a maximum at this juncture. The region above the F_2 peak is denoted the topside ionosphere, characterized by fully ionized plasma (*Schunk and Nagy*, 2009).

The protonosphere or plasmasphere is the doughnut shaped region around the Earth, collocated and above the topside ionosphere characterized by high concentrations of H+ ions (*Schunk and Nagy*, 2009). The altitude range of GAIM-GM encompasses part of the plasmasphere.

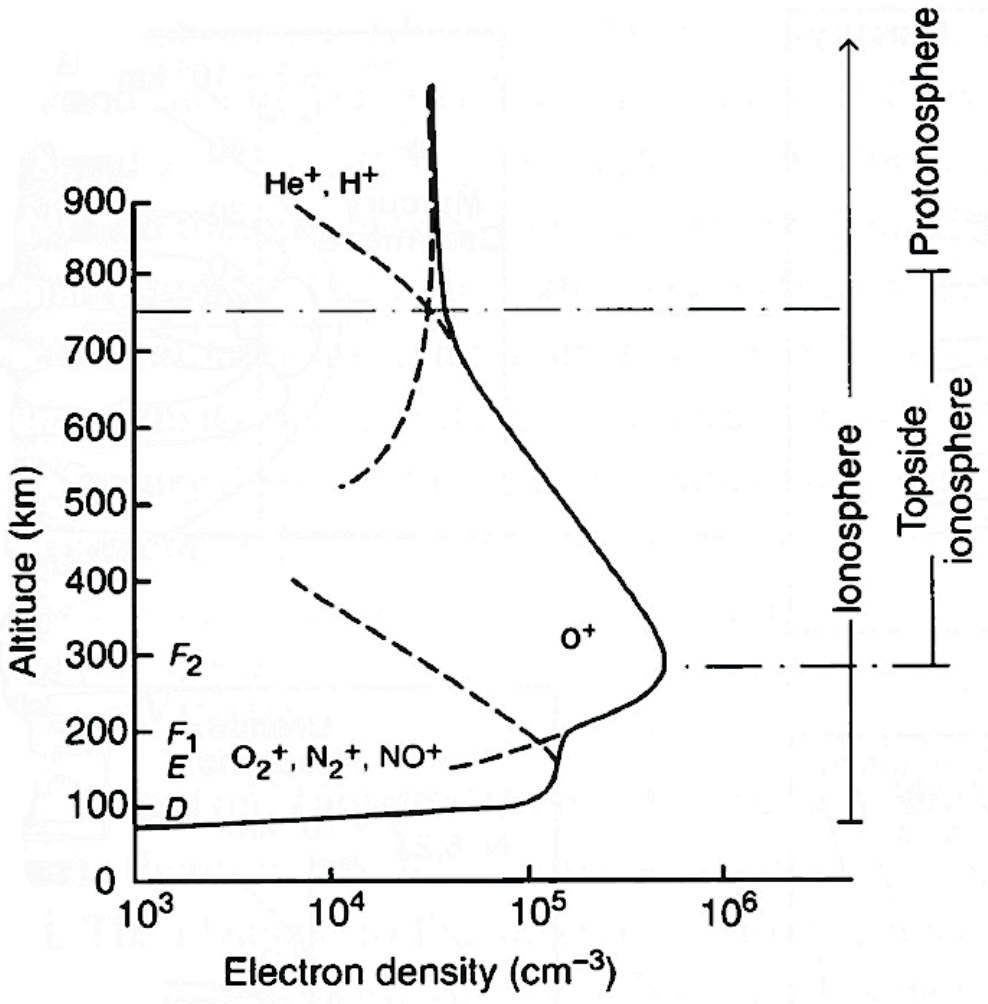

Figure 1. Ionospheric profile for selected ions and electrons as well as the layers of the ionosphere. (Adapted from Schunk and Nagy, 2009)

2.2 GAIM-GM

The GAIM-GM model is a time dependent physics based model that uses the Ionospheric Forecast Model (IFM) as a background model upon which perturbations are imposed via a Kalman filter data assimilation scheme. GAIM-GM can use either real time or historical data to generate ionospheric specifications as well as forecasts up to 24 hours out from the current specification (*Scherliess et al*., 2006).

GAIM-GM outputs three dimensional ion and electron densities of the ionosphere at altitudes from 90 km to 1400 km at 15 minute time intervals as well as total electron content (TEC), peak density of the F_2 region (NmF_2) and height of the F_2 peak (h_mF_2). TEC is the total number of electrons between two points given in units of electrons/m^2, for example, between a satellite and a ground based GPS receiver, and is sometimes reported in TEC units (TECU), with one TECU equivalent to 10^{16} electrons/m^2. GAIM-GM global resolution is 4.67 degrees latitude by 15 degrees longitude. Its vertical resolution is 4 km in the E region and 20 km in the F region, the same vertical output resolution as the IFM. GAIM-GM can also be run in a regional mode with a finer resolution (*Scherliess et al*., 2006).

GAIM-GM is able to assimilate many data types and is modular such that new data types will be able to be incorporated into the data assimilation scheme. Data that GAIM-GM can assimilate include in situ electron densities from governmental satellites, namely the Defense Meteorological Satellite Program (DMSP) and National Oceanic and Atmospheric Administration (NOAA) satellites, bottomside electron density profiles, and line of sight TEC measurements from thousands of ground stations and GPS satellites among others (*Schunk et al.,* 2004). The highlighted data types correspond to those that

are ingested in the operational model currently in use at AFWA. Other data that GAIM-GM can ingest but that are not currently used by AFWA include data from UV sensors aboard the DMSP satellites, measurements from various satellites to include the TOPEX satellite used in previous model verification studies, and COSMIC occultation data, among others. Figure 2 shows the data platforms that GAIM-GM can assimilate along with the steps involved in operating GAIM-GM and the relationships between the IFM, data, Kalman filter and outputs. The first step in GAIM-GM is to set forth the time and geophysical conditions of the model run. Next the IFM, or physics based model, is run to generate a background ionosphere. From here, data is ingested and assimilated. The background ionosphere, in conjunction with the assimilated data produces the current state ionospheric specification as well as forecasts from this specification out to 24 hours.

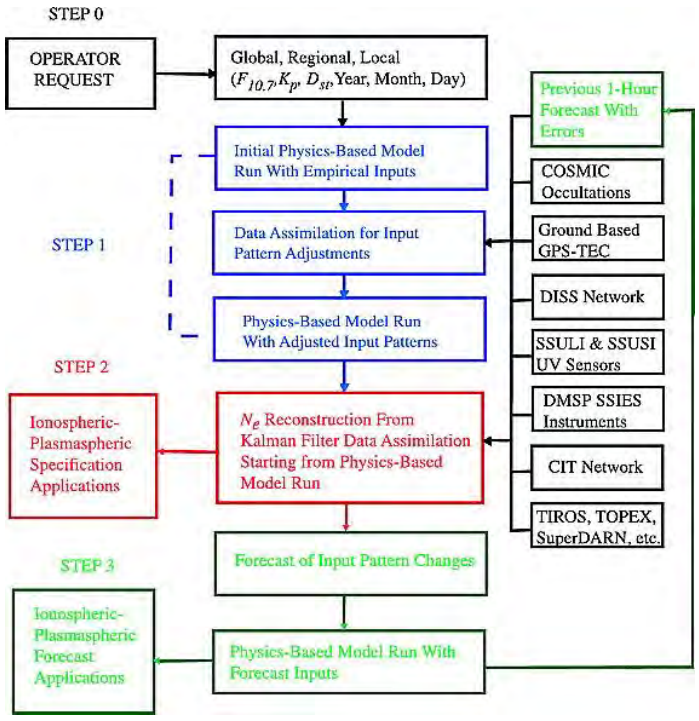

Figure 2. Flow chart of GAIM-GM operational sequence. Shown are the steps involved in operating GAIM-GM, data that can be assimilated, input parameters and outputs (Adapted from Schunk, 2004).

2.2.1 Ionospheric Forecast Model (IMF)

The Ionospheric Forecast Model is a physics-based numerical model of the global ionosphere. The IFM calculates time-dependent density distributions in three dimensions for the following ions: NO^+, O_2^+, N_2^+ and O^+, in the E region. It also calculates density distributions for the major ions, O^+ and NO^+ as well as for minor ions N_2^+ and O_2^+, in the F region. Electron and ion temperatures are also calculated in the E and F regions. Furthermore, H^+ densities are calculated in the F region and topside ionosphere (Schunk et al., 1997).

The IFM encompasses the region 90 km-1400 km above the earth with a spatial resolution of 4 km in the E region and 20 km in the F region. Using either geographic or geomagnetic coordinate systems, the IFM generates density and temperature outputs at a resolution of 3 degrees latitude by 7.5 degrees longitude (*Schunk et al.,* 2004).

The IFM needs only several basic input drivers to run. These include $F_{10.7}$ solar flux proxy number (indicates the level of solar activity), year, day, start time, duration and 3 hourly Kp values (indicates level of geomagnetic storming) from 3 hours prior to the start time through the end of the model run (*Schunk et al.,* 2004). Due to its dependence on these simple drivers as well as empirical models to derive the output, the IFM is more representative of the ionospheric climatology than it is for shorter term weather variations (*Sojka et al.,* 2007).

The output obtained from IFM is the result of the numerical solutions to the energy, momentum, and ion and electron continuity equations. The physical processes taken into account in this model are the following: (1) field aligned diffusion due to density and temperature gradients, gravity and the ambipolar electric field, (2) cross field

electrodynamic drifts due to the magnetopsheric and dynamo electric fields, (3) ion production from UV and solar radiation, resonantly scattered solar radiation, starlight, and auroral electron precipitation, (4) numerous energy dependent chemical reactions, (5) thermospheric winds, (6) neutral composition changes, (7) thermal conduction, (8) many elastic and inelastic heating and cooling processes. Also, the geomagnetic and geographic polar offset is accounted for in the IFM (*Schunk et al.,* 2004).

2.2.2 Data

GAIM-GM can assimilate a wide variety of data types. The operational model run at AFWA currently ingests three types: GPS slant TEC, bottomside electron density profiles obtained from ionosondes, and in situ electron density readings from DMSP satellites from the Special Sensors-Ions, Electron, and Scintillation (SSIES) instrument. The quantity of data ingested can also be controlled by editing the lists of GPS ground sites and ionosonde sites that GAIM-GM is programmed to accept as well as specifying the DMSP satellites from which to accept data.

2.2.2.1 GPS

Data obtained from GPS is extremely valuable due to the spatial and temporal coverage that it provides. GPS consists of both satellite and ground based stations that communicate through the ionosphere. In obtaining proper time and location measurements, GPS must take into consideration the ionospheric environment and does so by computing the electron content in the path between satellites and ground based receiving stations. This is accomplished by detecting the time delay from two radio signals of different frequency between the satellite and the ground receiver and relating this to electron density (*Ondoh,* 2001). These electron readings are called slant TEC and

can be obtained and assimilated in near real-time. They are also archived by NOAA and made available from their Continuously Operating Reference Station (CORS) website. Ground based GPS receivers may be in contact with more than one satellite at a time and may therefore provide more than one slant TEC measurement at a time.

2.2.2.2 Ionosonde

An ionosonde is a type of radar that transmits radio waves of different frequencies into the ionosphere. The waves are reflected at the point where the radio frequency transmitted equals the plasma frequency of the ionosphere. The radio waves then travel back and are picked up by the receiver. From the time difference between the transmission and reception of the radio wave, a height is obtained. If the propagation speed is assumed to be the speed of light, then the height is virtual. To obtain the actual height of reflection, the group velocity of the propagating wave must be determined. The electron density at this height is determined via the plasma frequency equation given by

$$f = \sqrt{\frac{e^2 n_e}{4\pi^2 m_e \varepsilon_o}} \tag{1}$$

Where f is the frequency, e is the electron charge, n_e is the electron density, m_e is the mass of an electron and ε_o is permittivity (*Ondoh,* 2001). A bottomside electron density profile of the ionosphere is obtained from the ionosonde and GAIM-GM assimilates this data.

2.2.2.3 DMSP

The Defense Meteorological Satellite Program satellites are part of a government run satellite program that observe the earth, oceans and study their physical processes. These satellites are sun synchronous polar orbiting satellites that fly at an altitude of ~830 km and are equipped with several types of sensors. The Special Sensors-Ions, Electron, and Scintillation (SSIES) instrumentation aboard these satellites collect in situ ion and electron density readings that are input into GAIM-GM. This is done with a suite of sensors located on the satellite that include a retarding potential analyzer, ion drift meter, a scintillation meter, and a Langmuir probe. These sensors work together to determine the flow, temperature, angle and current of the plasma in the ambient satellite environment. From these sensors the electron density is measured and this data is input into GAIM-GM (*Delorey et al*., 1989).

2.2.3 Kalman Filter

Data quality and availability for the space environment continue to increase, making space weather data assimilative models more reliable. In order to leverage the data to improve the model accuracy of GAIM-GM, a Kalman filter data assimilation scheme is used. The data ingested into GAIM-GM is run through the Kalman filter, adding ionospheric perturbations to the IFM to generate more accurate specifications and forecasts (*Scherliess et al*., 2006).

The Kalman filter is a sequential least squares (best fit) procedure that is expert in taking in various data types into the model and properly assigning confidence to each data assimilated. The data is used to further refine the specification from which the forecast is generated (*Howe,* 1998). When inputting data into the model, it is necessary

to associate errors with the ingested data. For GAIM-GM, a statistical Gauss-Markov model from a background error covariance matrix is used. This matrix was derived from 1107 separate 2 day runs of IFM taken from varying ionospheric drivers and geomagnetic conditions (*Thompson et al.*, 2006).

2.3 Skill Score

A common measure in determining the accuracy of any forecast model is the use of a model skill score. Three components are needed to generate a single skill score. These typically take the form of a forecast, an observation and a reference. The idea is to compare both the forecast and a reference (typically climatology) to an observation to determine which is more representative, in this case with respect to the ionosphere. This forecast skill is computed by comparing the root mean square error (RMSE) between the forecast and the observation to the RMSE between the reference and the observation. The first RMSE compares the error between the forecast and the observation through the following equation

$$RMSE = \sqrt{\frac{1}{\mathrm{M}} \sum_{m=1}^{\mathrm{M}} (\mathrm{F}_m - \mathrm{O}_m)^2} \tag{2}$$

Where F denotes the forecast and O denotes the observation. The second compares the error between the reference and the observation as given by

$$RMSE_{ref} = \sqrt{\frac{1}{\mathrm{M}} \sum_{m=1}^{\mathrm{M}} (\mathrm{R}_m - \mathrm{O}_m)^2} \tag{3}$$

Where R is the reference and O is the observation. The skill score is then derived from these two errors by the equation

$$\text{Skill Score} = 1 - \left(\frac{\text{RMSE}}{\text{RMSE}_{\text{ref}}} \right) \tag{4}$$

Skill scores are therefore bounded by 1 for a perfect forecast as this indicates perfect agreement between the forecast and the observation. Skill scores approach an undefined value or get largely negative when the reference is more representative than the forecast. Therefore, skill scores greater than zero imply that the forecast was more representative than the reference when compared to the observation. A zero skill score indicates that the model forecast and the reference were equivalent in their representation, and a negative score states that the reference was more representative than the forecast output (*Wilks,* 2006). The choice for the reference is important as models and references have inherent strengths and weaknesses that must be taken into consideration when computing skill scores. In other words, some models favor climatology while others focus in on more short term weather phenomena.

2.4 Previous Validations

This section outlines some of the notable previous work with regard to GAIM-GM specifications and forecast validation. Also included is a summary of work done by Thompson et al. (2006) regarding model specification accuracy given various data inputs. The objectives are to outline what has been done previously to vet the output quality of the model, to determine GAIM-GM specification accuracy and use that as a benchmark for comparisons in this work, and to illuminate the need to properly verify GAIM-GM model forecast accuracy.

2.4.1 Specification Validation

Various validation studies to determine the accuracy of the specification of GAIM-GM have been carried out by both AFRL and USU. The team at AFRL tested operationally significant parameters that include the maximum usable frequency (MUF) for HF communications. Because it is impractical and very difficult if not impossible to ubiquitously measure the entire ionosphere, the validation and verification studies of GAIM-GM have typically focused on point locations or been compared to climatologically based empirical models. For example, AFRL validated the MUF over Australian ionosonde sites and compared GAIM-GM output with these ionosonde measurements as well as to climatologically based monthly median MUF. They found that GAIM-GM errors for monthly median MUF values were 10% for daytime and 16% at night (*McNamara et al.*, 2008).

Utah State University, likewise, has conducted validation studies of GAIM-GM. Zhu et al. (2006) published a comprehensive validation study comparing GAIM-GM output to TEC measurements obtained from the TOPEX satellite. The TOPEX satellite

was launched on August 10, 1992, and its main mission is to determine sea surface heights. Because TOPEX is a nearly sun synchronous satellite that orbits the earth at ~1350 km, it is well placed to determine TEC for the same range of the ionosphere as IFM. The look path from TOPEX to the Earth encompasses much of the ionosphere making it suitable as an observational tool. The satellite is equipped with two dual-frequency altimeters and from this instrumentation TEC estimates are obtained. The TEC comparisons were made between TOPEX and IFM, the physics based background model for GAIM-GM. It should be noted that the validation in this case is not explicitly for GAIM-GM but rather the GAIM-GM background. The results indicate that the IFM and TOPEX TEC measurements are consistent, with daytime readings outperforming nighttime. Quantitatively, the TEC differences are typically below 20% with some values within 10% (*Zhu et al*., 2006). The 80% – 90% agreement between the TOPEX TEC measurements and IFM is the basis for using GAIM-GM specifications as the observation for the skill score comparisons.

2.4.2 Data Impacts

Since GAIM-GM is able to assimilate various types and quantities of data, it is important to determine how changes in data type and quantity alter the output specification and forecasts. Note that GAIM-GM can also be run with no data ingested and in this case the IFM background and error covariance matrix derived from a set of 1107 IFM runs creates an ionospheric climatology output. Thompson (2006) investigated such impacts due to data variations by running GAIM-GM for five scenarios with varying combinations of both GPS TEC data and ionosonde electron density profiles. These data combinations were run over a 30 day period and compared to TOPEX TEC

measurements and also compared to ionosonde electron density profiles from Bear Lake Observatory in Northern Utah. It was found that combining GPS and ionosonde data created more accurate results than simply using one type of data and not another. Furthermore, increasing GPS data without increasing the output grid spacing may have a negative impact on model accuracy (*Thompson et al.*, 2006). Thompson's work did not include the impact of DMSP data on model specification accuracy. Investigations into forecast accuracy from various combinations of data ingests are included in the recommendations section. Nevertheless, in an effort to use the most representative specification for model accuracy analysis, GPS, ionosonde and DMSP are used in the specification.

III. Methodology

This chapter discusses the methods used in carrying out the research. Sections within the methodology include: (1) specifying the geophysical conditions of the model cases, (2) running the IFM, (3) obtaining input data and reducing it into useful forms, (4) choosing the data locations to be ingested, (5) running GAIM-GM, (6) changing the output grid to focus on CONUS, (7) how the comparative analysis are carried out.

3.1 Geophysical conditions

GAIM-GM was run for four different cases with varying geophysical conditions. The dates, geomagnetic storming conditions (Kp values), and solar activity ($F_{10.7}$) values for each case are set forth in Table 1. These four cases produce GAIM-GM output from geomagnetic quiet conditions (low Kp) and storming conditions (high Kp) as well as solar min (low $F_{10.7}$) and solar max (high $F_{10.7}$). Table 2 shows the relationship between Kp values and geomagnetic storming conditions. Geomagnetic storms alter the ionosphere by enhancing the ionospheric electrical currents via incoming energy and plasma ejected from the sun. An enhancement in ion densities and fluctuations or the disappearance of the F_2 peak may result from these storms and thereby impact space based capabilities.

Table 1. Geophysical conditions and dates for the four cases investigated.

Case	Days	Year	Geomagnetic Activity (Kp)	Solar Activity ($F_{10.7}$)
1	211-213	2010	Quiet (2)	Minimum (84)
2	215-217	2010	Moderate Storm (6)	Minimum (83)
3	95-97	2010	Strong Storm (7)	Minimum (78)
4	170-172	2001	Quiet (3)	Maximum (205)

Each of the four scenarios was run to produce three days of reliable output. The quiet geomagnetic conditions during solar minimum are taken from days 211-213 (case 1) in 2010. The geomagnetic storming cases are for days 215-217 (case 2) and days 95-97 (case 3) in 2010 and correspond to moderate and strong geomagnetic storms respectively. Quiet geomagnetic activity during solar maximum conditions is taken from days 170-172 (case 4) in 2001. Case 1 and case 2 run nearly consecutively. This is by design as both cases are therefore taken from the summer time. This helps to eliminate the seasonal variation associated with the ionosphere. Since the onset time of geomagnetic storms varies from storm to storm, two geomagnetic storms were investigated. Case 2 and case 3 were chosen as their storm onset times are offset by ~9 hours. This approach enhanced the investigation on model forecast accuracy during geomagnetic storms.

Table 2. Geomagnetic storming conditions related to Kp values, adapted from SWPC website (http://www.swpc.noaa.gov/NOAAscales/index.html#GeomagneticStorms)

Kp Index	Storm Strength
5	Minor
6	Moderate
7	Strong
8	Severe
9	Extreme

3.2 Running IFM

Because the IFM provides the background upon which the ionospheric perturbations are imposed in GAIM-GM, the IFM must be run and this background ionosphere must be in place before running GAIM-GM. The input parameters needed to

run IFM include year, Julian day, Kp value, $F_{10.7}$ and $F_{10.7A}$ (81 day $F_{10.7}$ running average).

The IFM requires a 24 hour warm up period before reliable data is obtained as the IFM uses output from the previous day to generate current output. Furthermore, the IFM must be run for a sufficient duration as the forecast output for GAIM-GM likewise need background IFM data (i.e. specification and forecasts both need IFM background).

3.3 Data Acquisition and Format

With the background IFM in place, the attention turns to the data ingested into GAIM-GM. The overall process can be summed up in two steps. (1) Obtaining the raw GPS, ionosonde, and DMSP data and (2) formatting the data to a user friendly version that GAIM-GM will accept.

3.3.1 GPS Data

Ingested GPS data are acquired from the Continuously Operating Reference Station (CORS) database maintained by NOAA. This data is packaged as Receiver Independent Exchange Format (RINEX) files. Once obtained, the files are stored and formatted such that GAIM-GM can ingest the time, satellite location, ground station location, phase TEC and phase TEC error.

3.3.2 Ionosonde Data

Ionosonde data was obtained from the National Geophysical Data Center (NGDC) database and contains raw electron density profile data. This raw data is then formatted into a data text file containing the essential components for the electron density profile that GAIM-GM will ingest. The formatted data includes best estimate NmF_2 and h_mF_2,

uncertainties in those parameters, latitude and longitude of the ionosonde site as well as electron densities for select altitudes and their uncertainty.

3.3.3 SSIES Data

The SSIES data from the DMSP satellites was obtained from the NGDC as well as provided by Dr. Daniel Ober and Dr. Gordon Wilson from the Air Force Research Laboratory (AFRL). The final output used by GAIM-GM contains the time, location, electron density and uncertainty of the measurements taken from the satellite.

3.4 Data Retention Lists

The number and locations of ingested data can be specified for each model run. This is done by changing the station retention lists located within the directory from which GAIM-GM is run. Both specification and forecast output was used to determine forecast accuracy. Therefore it was necessary to run GAIM-GM several times for each case, each with different station retention lists in order to obtain the most representative forecasts and specifications for use in the forecast accuracy analysis. The details of the GPS and ionosonde lists used are discussed in the following sections. All available SSIES data from DMSP satellites F16, F17 and F18 were used in cases 1-3 while all SSIES data from DMSP satellites F13, F14 and F15 were used in case 4. The model was also run with no data ingested, and results from these runs comprise the ionospheric reference background needed for the skill score and forecast accuracy analysis.

3.4.1 AFWA Data List-Forecast

To closely mimic GAIM-GM forecasts, as run by AFWA, it was necessary to obtain the lists of both GPS and ionosonde stations that AFWA currently uses when running the model. GAIM-GM can be programmed to accept data from many locations

but AFWA only uses a small subset of the total available data. Lists of 59 GPS stations and 17 ionosonde sites, visualized in Figure 3, ingested by AFWA during February 2011, were used in the GAIM-GM model runs to duplicate AFWA forecasts. The forecast output generated from GAIM-GM runs from these lists is the forecast data used in the computation of the skill score.

3.4.2 All Data List-Global Specification

To properly evaluate global AFWA forecast grids discussed in the previous section, a globally representative specification was used. This specification was obtained from a list of 351 GPS sites from around the world, generated by a program developed at USU. This program generates a global distribution of ingested GPS sites. The ingested ionosonde data is comprised of 49 worldwide ionosonde sites that GAIM-GM at AFWA is programmed to ingest. Representations of these data sites are seen in Figure 4. Recall that only 17 of these sites were ingested in the AFWA forecast run. The specifications from these runs are the global observations used in determining global skill scores.

3.4.3 AFWA and CONUS Data List – CONUS Specification

To properly analyze GAIM-GM forecast output over CONUS, a representative CONUS specification was used. The GPS data list for this case, visually represented in Figure 5, includes one GPS ground station for each grid point in the 7 by 5 array that encompasses the CONUS area with 30 of the 35 grid points represented. The GPS ground stations chosen over CONUS in this scheme are different than the GPS ground stations used in the AFWA ingest forecast list with the exception of Bermuda, as this location was used in both cases to allow greater data coverage over otherwise data sparse regions in the Atlantic Ocean. GPS ground based stations outside of CONUS are identical

to those of the AFWA data ingest list. The 17 ionosonde sites from the AFWA list were used in these runs.

3.5 Running GAIM-GM

Once the IFM runs are completed and the data is retrieved and formatted, GPS satellite and ground based station biases must be downloaded. The biases, which may stem from hardware limitations and calibration errors, and the uncertainty in the biases, are given in nanoseconds. Correcting for these biases increases the level of accuracy of the TEC measurements obtained from GPS.

The next step is to ensure that the configuration files that specify the start time, duration, forecast increments and range of the output as well as the desired data to be ingested are accurate. GAIM-GM can generate forecasts valid from 15 minutes to 24 hours from the current specification in 15 minute increments.

It is important to understand how and in what order GAIM-GM output is generated. Specifications are generated from the IFM background and the data ingested via the Kalman filter. A forecast suite is then generated from each specification. For the runs completed in this study, 3, 6, 12 and 24 hour forecasts are obtained from each specification and saved in directories that contain only those hourly forecasts (3-hour forecasts are saved together and 6-hour forecasts are saved together and so forth).

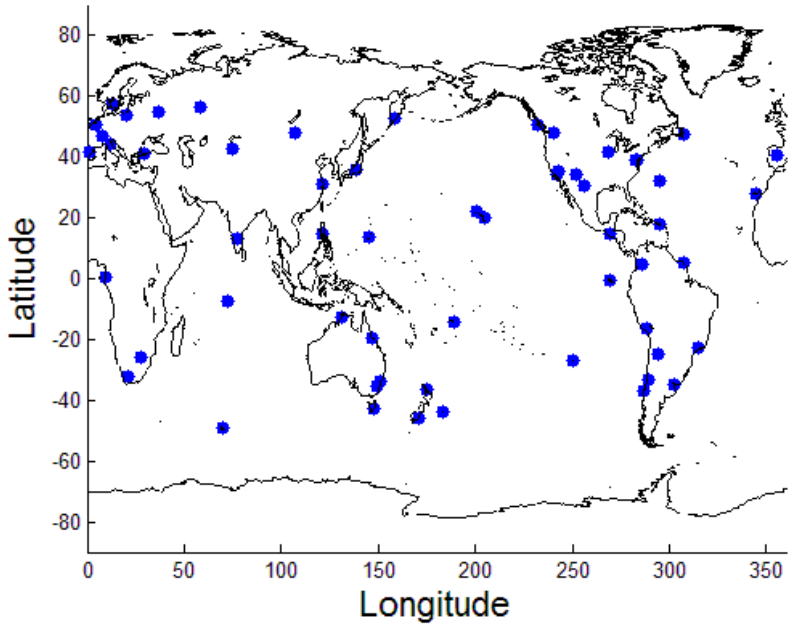

(a) GPS Sites

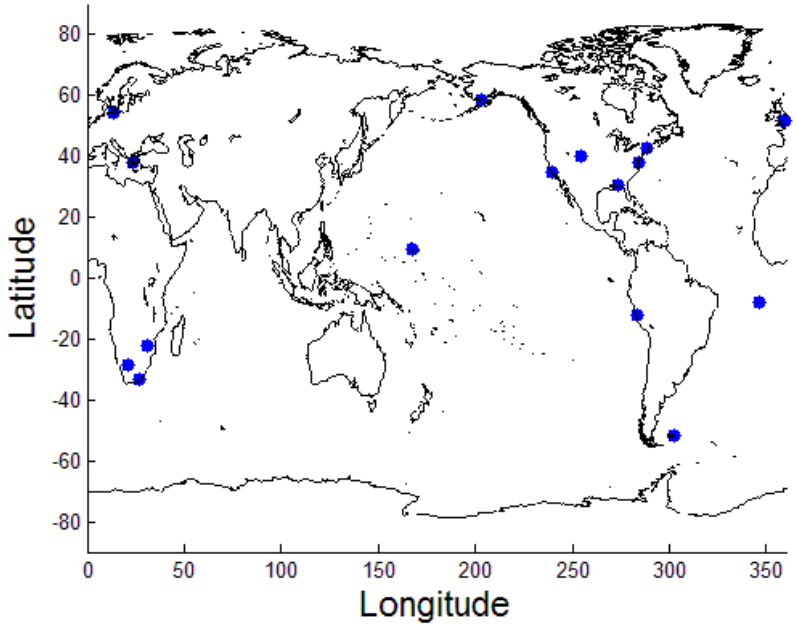

(b) Ionosonde Sites

Figure 3. AFWA data ingest sites: (a) GPS sites (59), (b) ionosonde sites (17). The forecast output used in the accuracy analysis is obtained from running the model with these sites ingested into the model.

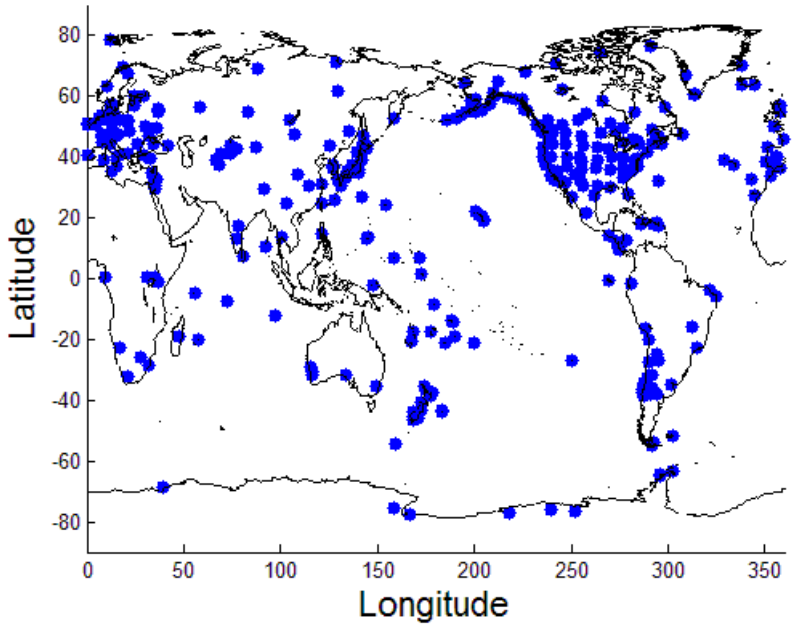

(a) GPS Sites

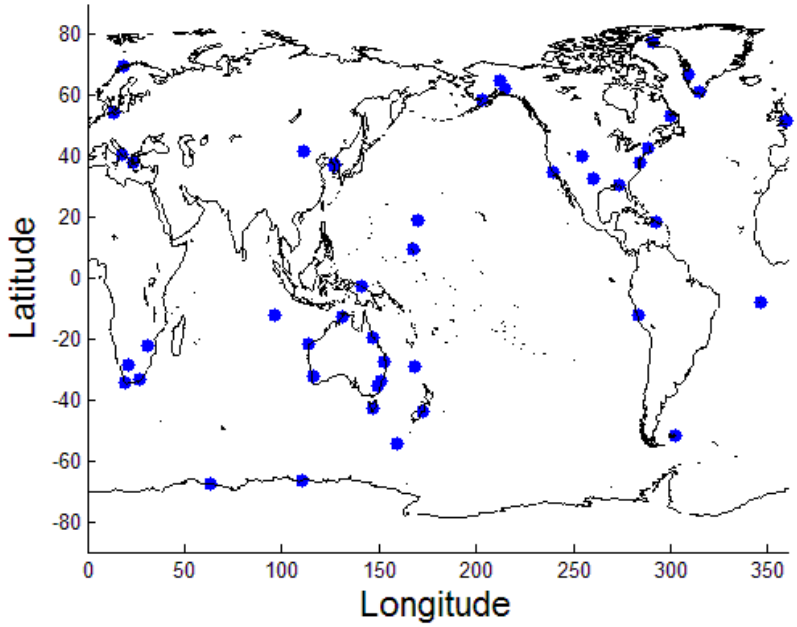

(b) Ionosonde Sites

Figure 4. All data ingest sites: (a) GPS sites (351), (b) ionosonde sites (49). The global specification output used in the accuracy analysis is obtained from running the model with these sites ingested into the model.

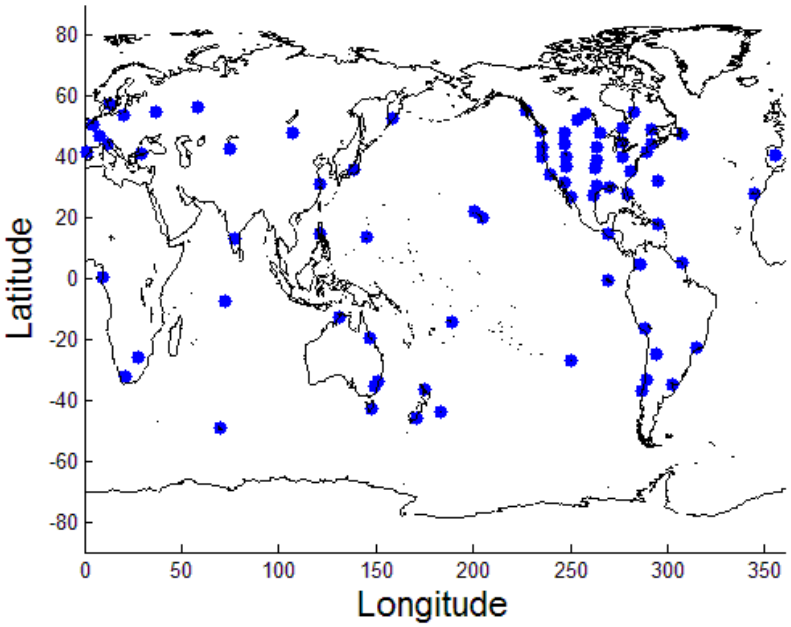

(a) GPS Sites

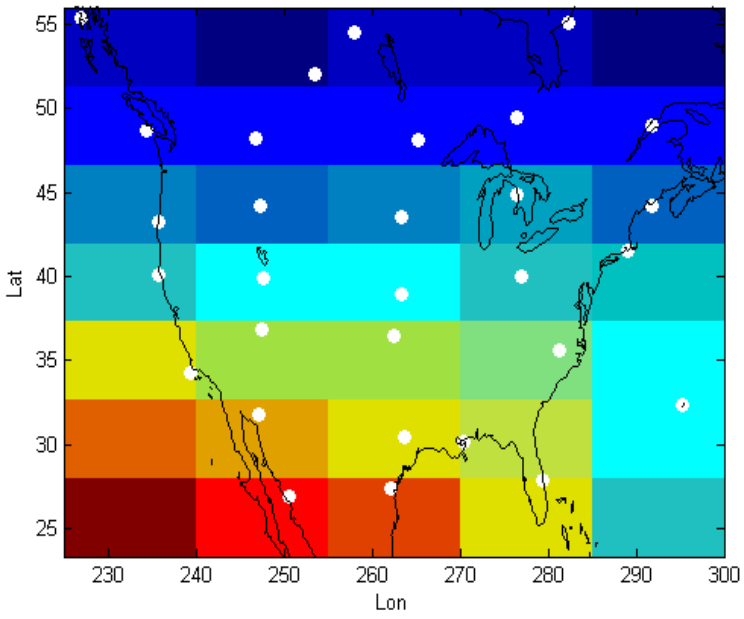

(b) CONUS GPS Sites

Figure 5. The AFWA plus CONUS data ingest sites: (a) GPS sites (79), (b) CONUS GPS sites (30). The CONUS specification output used in the accuracy analysis is obtained from running the model with these sites ingested into the model.

Once all the forecasts generated from a specification are saved, the model moves forward 15 minutes to the next specification and generates the next suite of forecast outputs. The forecast output files contained within their respective directories are the forecasts valid at the time indicated on their file name. The file naming convention includes the letters GMF, followed by the year, Julian day, hour, minute and netCDF file extension, for example, GMF20102110000.NC. This file would be valid at 0000UT on day 211, year 2010. A 24-hour forecast generated from a specification at a certain time is valid 24 hours from the specification time. A forecast variable is included in the netCDF file that indicates the number of seconds out from the specification for which the forecast is valid. Thus a forecast variable indicating 86400 seconds is a 24-hour forecast.

Recall that GAIM-GM was run for four cases of various geomagnetic and solar activity. Each case was run four times giving output corresponding to: forecasts obtained from the AFWA retention list, global and CONUS specifications obtained from the All and AFWA plus CONUS retention lists respectively, and reference output obtained from running the model with no data ingested.

3.6 Statistical Analysis

Several different types of statistics and plots were generated to carry out the analysis of GAIM-GM forecast accuracy. These include plots of TEC and TEC percent difference as well as forecast mean percent differences, RMSE and skill score values.

3.6.1 TEC and TEC Percent Difference Plots

TEC plots and forecast TEC percent difference plots are the building blocks from which all other plots and statistics are derived in this study. The graphical representations of TEC are taken directly from the TEC output from GAIM-GM. The

forecast TEC percent differences are computed by formula 5 where the differences are taken between corresponding grid points from the forecast and specification TEC outputs. Therefore, forecast TEC percent difference plots maintain the dimensions of the arrays from which they are derived. Furthermore, only one forecast TEC percent difference can be computed for each time step. An example percent difference plot is shown in Figure 6. Positive percent errors are denoted in red and those with a negative error are indicated in blue.

$$Percent\ Difference = \left(\frac{Forecast - Specification}{Specification}\right) * 100 \tag{5}$$

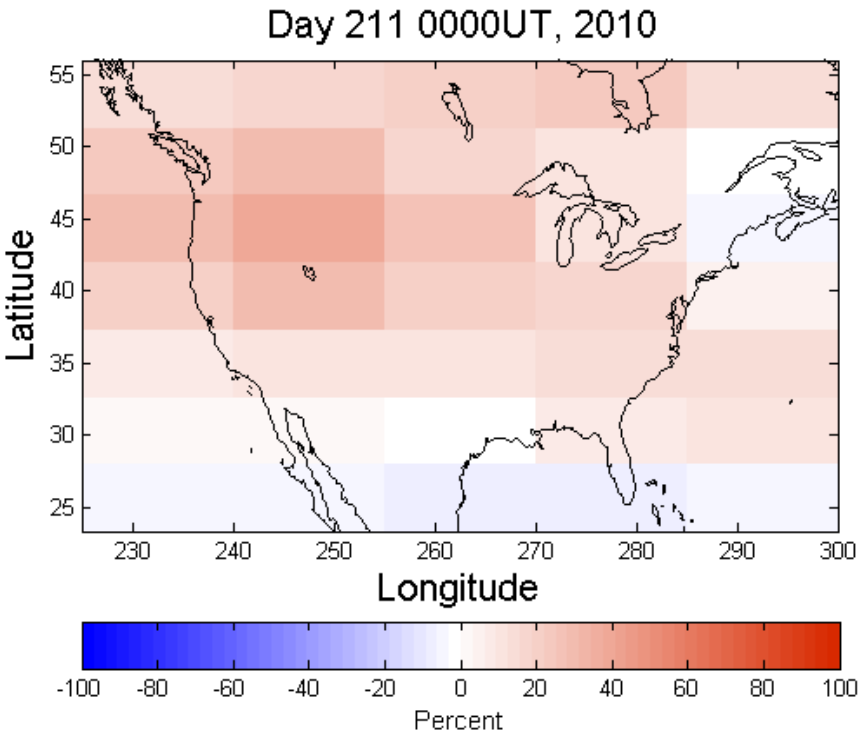

Figure 6. A forecast TEC percent difference plot. Each grid value is computed via equation 5, comparing corresponding forecast and specification grid points. Positive and negative percent differences are shown in red and blue respectively.

3.6.2 Mean Percent Difference

Mean percent difference (MPD) and mean absolute percent difference (MAPD) values were obtained by averaging the grid values from the forecast TEC percent difference arrays, such as those in Figure 6. The MPD simply averages the values of all grids within a forecast TEC percent difference plot. The MAPD takes the absolute value of each grid point in the forecast TEC percent different plot and computes the average of those values. The MPD and MAPD can be computed only once for each forecast TEC output. The MPD and MAPD were plotted together as line charts to depict the total percent difference as well as the positive and negative variations in the differences.

3.6.3 RMSE and Skill Score Value

Since the global output for the forecasts, specifications and reference are the same size (44 by 24 arrays), the global skill scores were straightforward to compute. The same can be said of the CONUS skill scores as the grid sizes for the components of the skill score were all 7 by 5 arrays.

Skill scores were generated for each forecast output (3-hour, 6-hour, 12-hour and 24-hour) for each of the four cases. The skill scores were computed using MATLAB and in accordance with the formulas specified in the background section.

GAIM-GM generates output every 15 minutes resulting in 96 outputs per day. Each case encompasses three days, providing 288 time increments from which skill scores were obtained and plotted. The forecast skill score shows how well the forecast compares to a reference. Recall that positive skill scores indicate an improvement over the reference whereas negative skill scores indicate that the reference was more representative of the ionosphere. It is important to understand that a negative skill score

does not necessarily indicate that the forecast was poor or inaccurate, only that the reference did a better job at specifying the ionosphere than did the forecast. It is possible to obtain excellent forecasts and negative skill score. It is also possible to obtain great errors in forecast output but maintain high skill scores. It is the ratio of the two RMSEs that indicate the skill score and not the absolute accuracy of the forecast.

The RMSE and RMSE reference, the building blocks of the skill score, were also plotted to show the overall error, trends in the error as well as the relationship between RMSE and skill score.

IV. Results and Analysis

The objective of this research was to determine GAIM-GM model forecast accuracy. This chapter presents the results and analysis of this investigation through the use of the skill scores and other statistics obtained from running GAIM-GM over various geophysical conditions. Four cases were investigated, first was a geomagnetic quiet, solar minimum case. The next two contained geomagnetic storming conditions during solar minimum. The fourth was during geomagnetic quiet, solar maximum conditions. This chapter analyzes forecast accuracy over both the entire globe and CONUS.

4.1 Global Forecast Trends and CONUS Focus

The global TEC forecasts were analyzed via the skill score and the forecast RMSE. A sample of 4608 values was obtained when combining the four cases, three days of output, the four forecast periods (3, 6, 12, 24) and the output cadence of 15 minutes. Of these 4608 values, only twice were negative skill scores obtained. These occurred for the 3-hour forecast output at 2115UT and 2130UT on day 95, 2010, case 3, with values of -0.0453 and -0.0048, respectively. The abundant positive skill scores show that globally, the forecast is virtually always more accurate than the reference.

The 3-hour global forecast skill scores and RMSEs for case 1 are plotted and shown in Figure 7. Although there are minor fluctuations in the skill score, the forecast RMSE and the reference RMSE shown in green, red and blue respectively, the overall variability is low. For example, the forecast RMSE range over the three days is 1.36 TECU with minimum and maximum forecast RMSE values of 1.23 TECU and 2.59 TECU respectively. A typical TECU forecast range for this case is from 0 to 40 TECU. The range, average, and standard deviation of the 3-hour forecast skill scores and forecast

RMSE for case 1 are included in Table 3. Similar results denoting low variability were obtained for cases 2-4.

Table 3. Range, average, and standard deviation for the 3-hour global forecast skill score and RMSE taken from case 1.

Global 3-hour Forecast Case 1	Skill Score	Forecast RMSE (TECU)
Range	0.33	1.36
Average	0.33	1.86
Standard Deviation	0.06	0.28

Global TEC forecasts show little variability in skill score and RMSE. This is likely due to the inclusion of data sparse areas such as the oceans and Africa that result in the forecast output reverting back to the specification background. It should be noted that high latitudes, those greater than 60 degrees, were omitted when determining global forecast accuracy as GAIM-GM does not assimilate data from these regions. Global output also masks the full extent of diurnal impacts and the impact of the Kalman filter in enhancing forecast accuracy. Therefore in order to determine the efficiency of the Kalman filter as well as the extent to which GAIM-GM can account for the diurnal pattern of the ionosphere, the data-rich CONUS area was selected for the remainder of the analysis.

4.2 Hourly Forecast Trends and 3-Hour Forecast Focus

GAIM-GM can forecast up to 24 hours from the current specification. The 3-hour, 6-hour, 12-hour and 24-hour forecasts were generated as part of this analysis. In reviewing the skill scores from these forecasts for each of the four cases, some overall trends were evident. Foremost among these was the consistent trend that the 3-hour skill scores outperformed all others. Figure 8 shows the CONUS skill scores for the four forecast periods obtained from case 1.

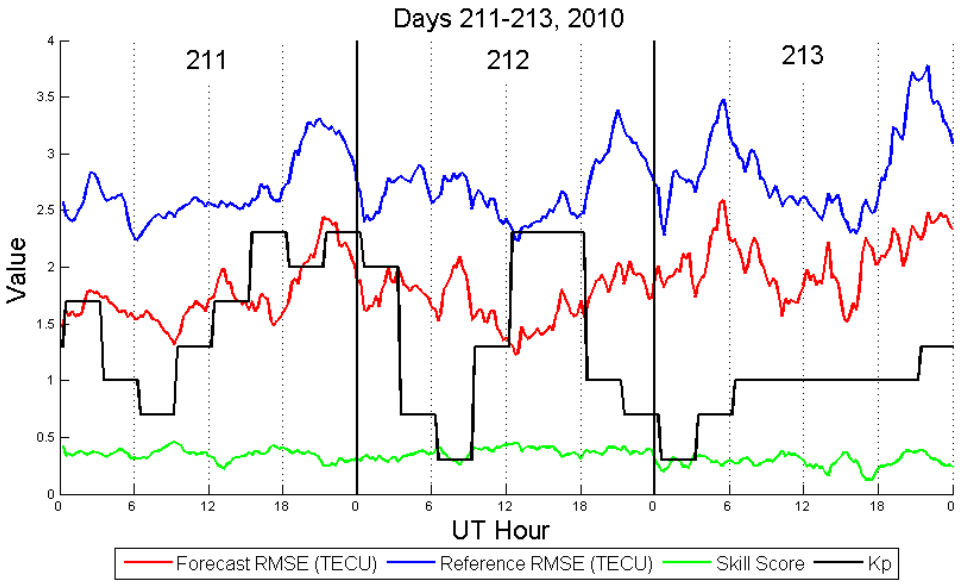

Figure 7. Global forecast skill score (green), forecast RMSE (red) and reference RMSE (blue) taken from the 3-hour forecasts for case 1, days 211-213, 2010.

The 3-hour forecast skill score, denoted in green is consistently greater than that of the other three forecasts. This is further illustrated in Figure 9, a bar chart of the average skill scores and average RMSE broken up by forecast period for all cases. Figure 9 indicates that as forecast range increases from 3 hours to 24 hours, the skill scores decrease and the RMSE increases. The average 3-hour forecast skill scores from case 4, for example, decreases from 0.51 to 0.28. The greatest RMSE difference is also found in case 4 when the RMSE increases from a 3-hour forecast output minimum of 3.86 TECU to 5.85 TECU at 24 hours. The high skill scores and high RMSE seen in case 4 are the result of the greater differences between the forecast and reference RMSE when compared to the other three cases. What is consistent however is that in the cases investigated, the average 3-hour forecast skill scores were greatest when compared to the other forecast periods. Furthermore, the 3-hour forecast RMSE were the least of the four

For this reason the 3-hour forecast output was chosen to be analyzed for the remainder of the study.

4.3 Case 1 Results

The baseline run for this study was taken from days 211-213 of year 2010. This mid-summer time period was characterized by quiet geomagnetic conditions during solar minimum. Also, a C3 solar flare was observed at 0826UT on day 213, but it did not impact CONUS data.

4.3.1 CONUS Skill Score

The 3-hour forecast CONUS skill scores for case 1 are plotted in green on Figure 10 along with the Kp values. The three day plot shows a decrease in skill score on each of the three days, centered near 06UT. The lowest skill score occurs on day 213 near 6UT with values as low as -0.42.

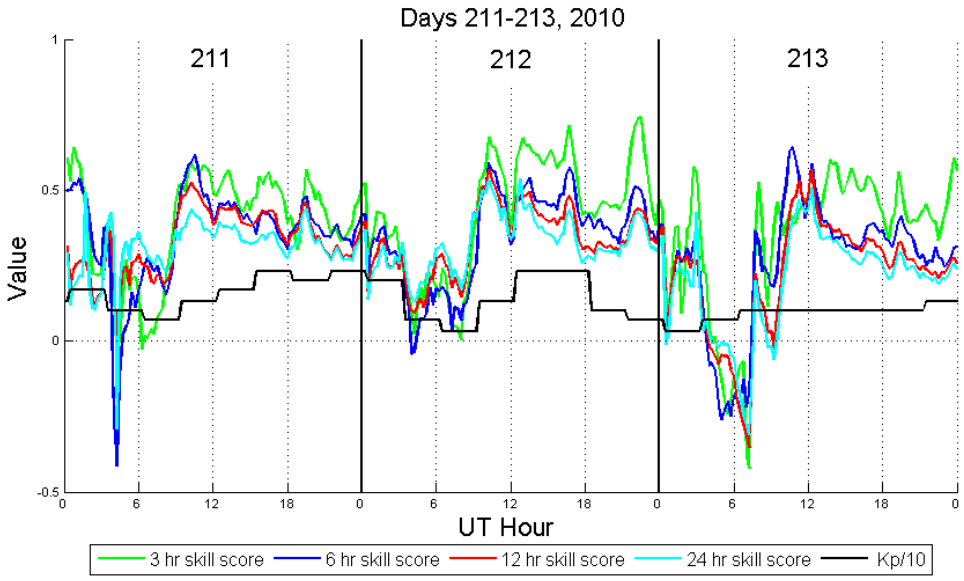

Figure 8. Forecast skill scores for all forecast periods obtained for case 1, days 211-213, 2010. Trending patterns are consistent among the four forecast ranges. Overall, the 3-hour forecast skill scores (green) are greater than the forecast skill scores obtained from the others three forecast periods.

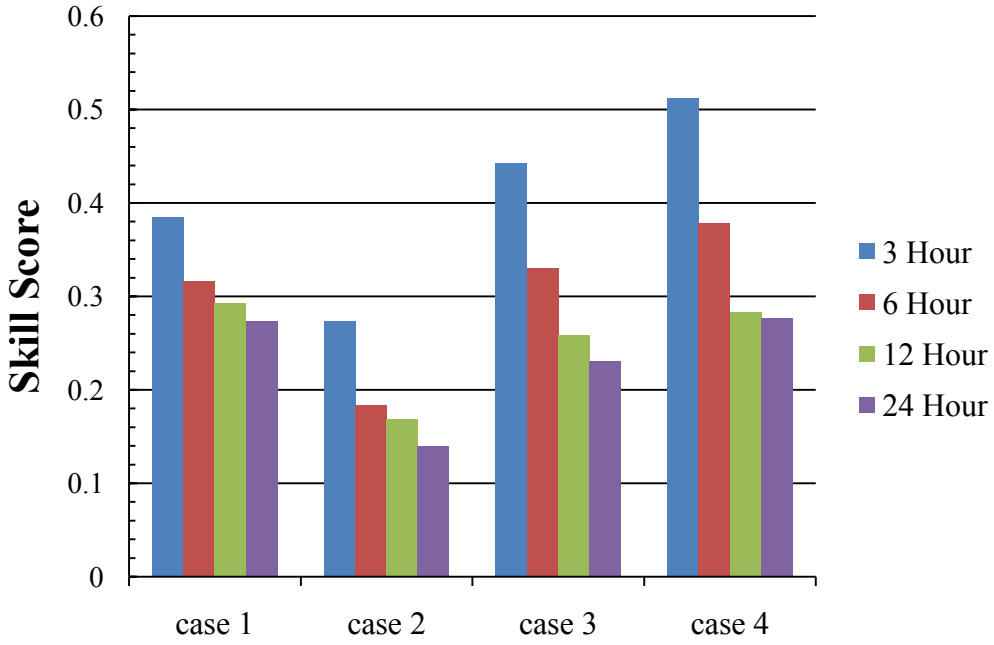

(a) Skill Score

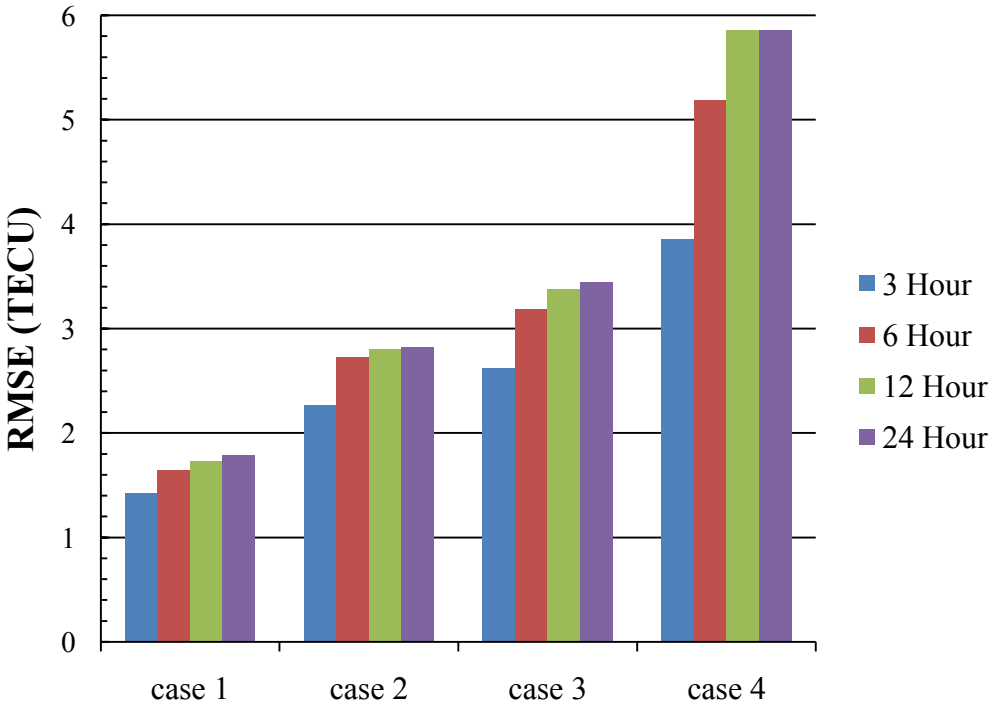

(b) RMSE

Figure 9. Bar charts showing (a) average skill scores for the four forecast periods for all cases and (b) average RMSE for all four forecast periods for each case.

Average skill scores were computed for both daytime (1300UT-2215UT) and nighttime (0330UT-0745UT) and are 0.49 and 0.06 respectively. The overall average skill score for the 3-hour forecast TEC output is 0.39.

The above average daytime skill score and the below average skill score at night indicates a diurnal trend in forecast accuracy. The RMSE was plotted to determine overall forecast error, to discern the trending in errors, and to further investigate the diurnal impact on forecast accuracy.

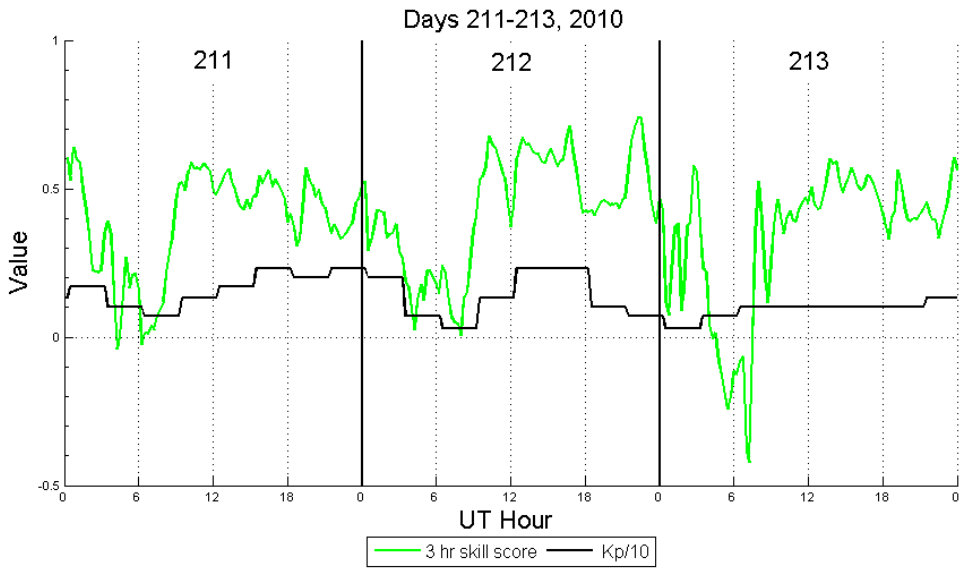

Figure 10. 3-hour forecast skill scores and Kp values for case 1, days 211-213, 2010. Kp values are reduced by a factor of ten to fit within the range of the plot. Note the decrease in skill score at night at 06UT for each of the three days.

4.3.2 CONUS RMSE

Forecast and reference TEC RMSE for the 3-hour forecast from case 1 were plotted in conjunction with the skill score and Kp values and are included in Figure 11. The forecast and reference RMSE, denoted by red and blue lines respectively, reach minima at ~06UT each day, consistent with the decrease in skill score seen in the green

lines in 10. Forecast and reference RMSE therefore appear to have a diurnal pattern. The forecast and reference RMSE not only increase during the daytime, but the difference between the forecast and reference RMSE also increases. Additionally, the range of the reference RMSE is greater than the range of the forecast RMSE. Both RMSEs remain near 1 TECU at night but the reference RMSE peaks at ~6 TECU on day 213 while the forecast RMSE peaks at ~3 TECU during the daytime on day 213. This is the reason for the rise in skill scores during the day, as the skill score is a function of the ratio of the forecast RMSE to the reference RMSE and not an indicator of the overall error associated with the forecast.

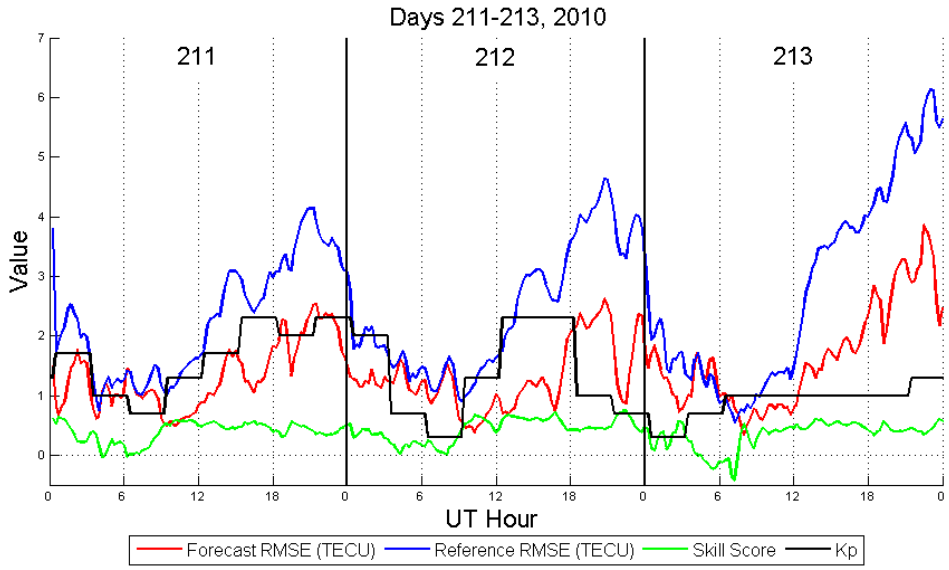

Figure 11. Forecast and reference TEC RMSE as well as skill score and Kp values for 3-hour CONUS forecasts from case 1. Where the skill score approaches zero is where the RMSEs are closest. The highest skill scores are found where the difference between the forecast and reference RMSE is the greatest.

4.3.3 CONUS MPD

The Mean Percent Difference and Mean Absolute Percent Difference (MAPD) between the forecasts and the specifications were computed. Whereas the RMSE is a

measure of the error, the MPD plots indicate the percent difference between the forecast and the specification. The MPD and MAPD were plotted together in blue and red respectively. Figure 12 shows the MPD which, like skill score and RMSE, also shows a diurnal trend with negative values at night and positive values during the day. The average daytime MPD, taken from the same time frame as the RMSE computation presented earlier (1300UT-2215UT), is 14.9%.

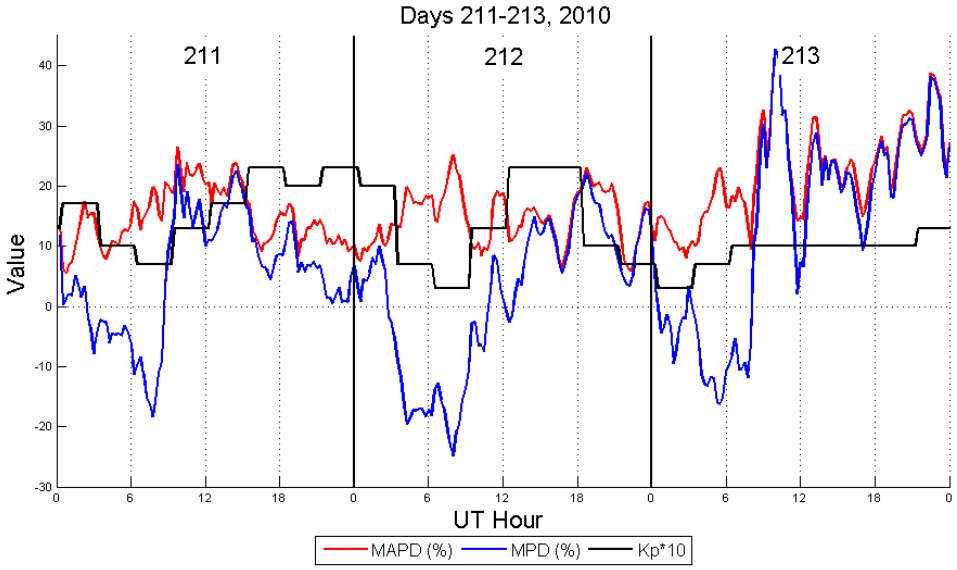

Figure 12. Mean Absolute Percent Difference (MAPD in red) and Mean Percent Differences (MPD in blue) for case 1, days 211-213, 2010. Note the distinct diurnal trend, with MPD values negative at night (0330UT-0745UT) and positive during the day (1300UT-2215UT).

The nighttime average MPD (0330UT-0745UT) is -12.3%. This indicates a negative forecast bias at night and a positive forecast bias during the day. A positive bias indicates that the forecast output was greater than the specification output whereas a negative bias indicates that the specification TEC values were greater than the forecast TEC values.

The daytime peak MAPD for days 211 and 212 are 25%, but the peak on day 213 is noticeably higher at above 40%. To investigate this, the FoF_2 critical frequency for

select CONUS locations for the same time frame is included in Figure 13. The FoF_2 parameter indicates the maximum frequency reflected by the ionosphere and is therefore a good indicator of the strength of the ionosphere and consequently of TEC. Higher reflected frequencies indicate increased plasma densities and therefore a stronger ionosphere. The slight decrease in FoF_2 on day 213 indicates that the ionosphere was likely weaker than the previous day. A greater forecast TEC value than observation TEC value would result in an enhancement in the positive bias and this shows up on the MPD plots for day 213.

4.4 Case 2 Results

Case 2 includes the three day period for days 215-217, 2010. Beginning two days after the end of case 1, this case is also during mid-summer. A geomagnetic storm with Kp values above 6 peaked at 22UT on day 215. The diurnal bias calculations for case 2 are from the same time range as those in case 1 as there is not a significant change in day and night durations between these two cases.

4.4.1 CONUS Skill Score

Skill scores for this case decrease during night as in case 1. Negative skill scores are observed at night for each of the three days in case 2. A negative spike in skill scores is also observed near 22UT on day 215, coincident with the peak in the storm and during daytime. This is shown on Figure 14, the plot of skill scores for case 2. The decrease at 22UT on day 215 is the result of the forecast RMSE being greater than the reference RMSE.

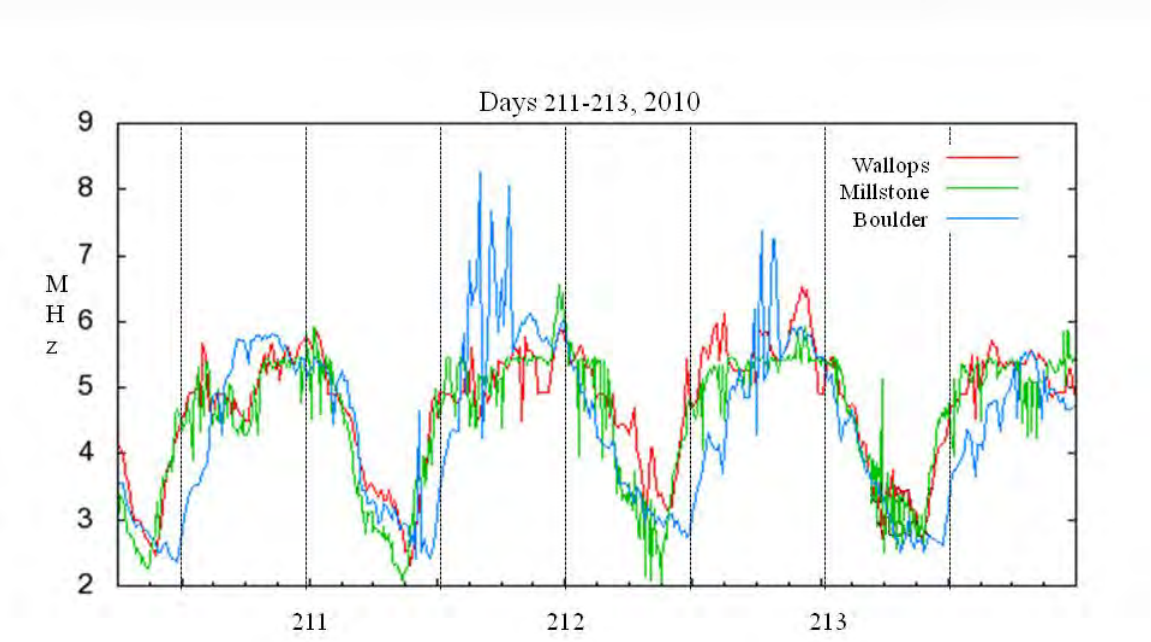

Figure 13. FoF_2 critical frequency plots for select CONUS locations during case 1, days 211-213, 2010.

4.4.2 CONUS RMSE

The RMSE plot for case 2, Figure 15, illustrates the diurnal pattern of RMSE increasing during the day and decreasing at night. It also shows the tendency for skill scores to decrease at night as the forecast and reference RMSE not only decrease, but become close to one another. In this particular case however, there are several deviations from what was observed in case 1, namely the overall increase in the magnitude of the RMSEs and the extreme peak in forecast RMSE in line with the peak of the geomagnetic storm at 22UT on day 215.

When compared to case 1, where the average forecast RMSE was 1.42 TECU, case 2 average forecast RMSE is 2.27 TECU, or a 59% increase. The forecast RMSE range more than doubles in case 2 from case 1, going from 0.34 TECU - 3.87 TECU for case 1 to 0.26 TECU - 8.36 TECU in case 2.

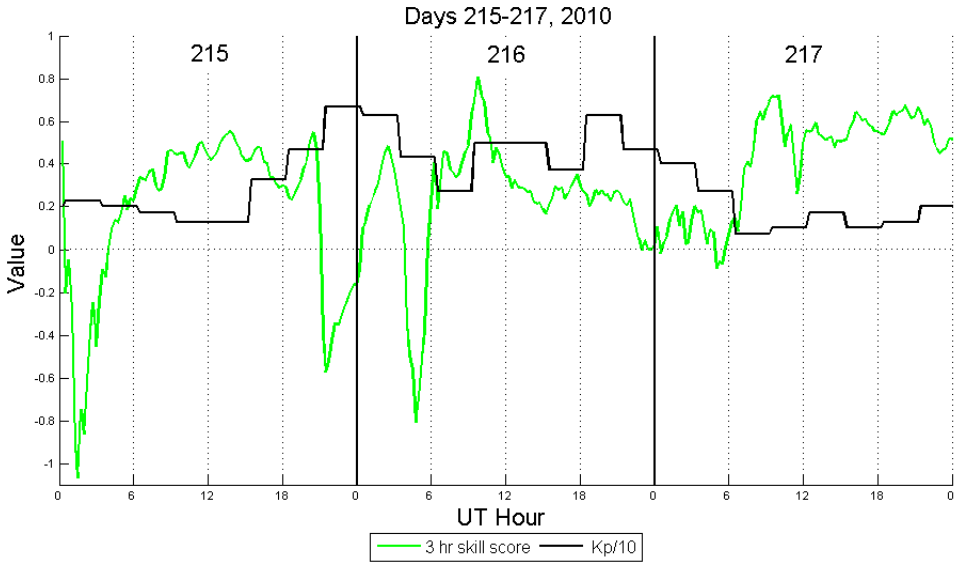

Figure 14. Skill scores and Kp values for case 2, days 215-217, 2010. Nightly decreases in skill score are present, as they were in case 1.

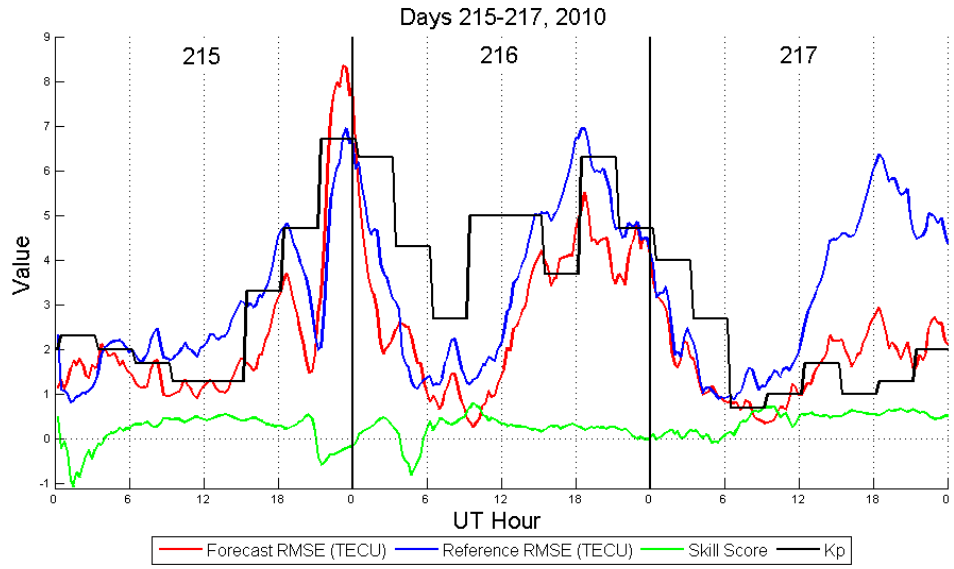

Figure 15. Forecast and reference RMSE as well as skill scores and Kp values for case 2, days 215-217, 2010. Diurnal peak in RMSE is in line with the peak of the geomagnetic storm.

4.4.3 CONUS MPD

The MPD plots for case 2 also indicate a diurnal bias to under forecast at night and over forecast during the day. The negative nighttime MPD values are seen in case 2

in Figure 16 as they were in Figure 12 for case 1. The average MPD at night is -7.6% compared to 25.0% during the day.

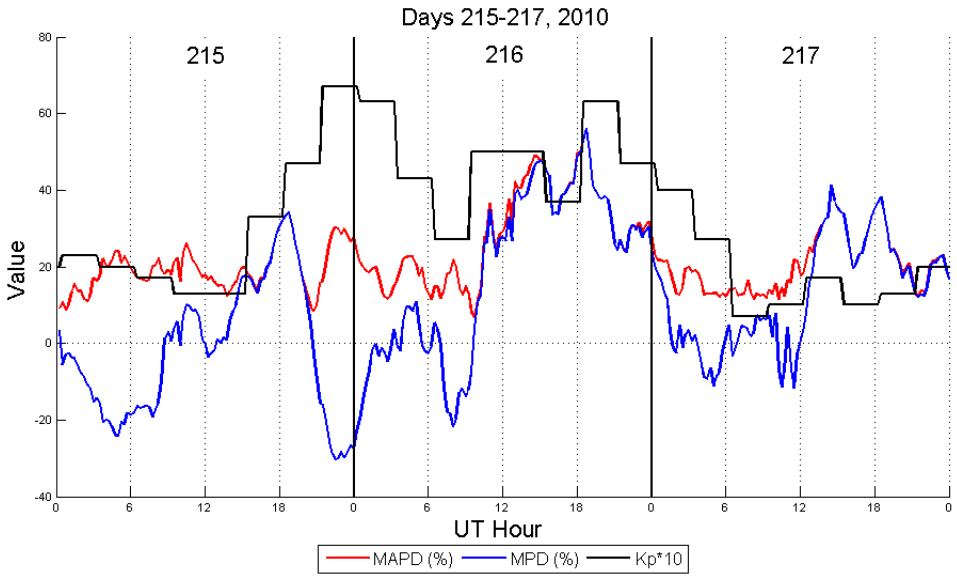

Figure 16. Forecast TEC MPD and MAPD values for case 2, days 215-217, 2010.

The geomagnetic storm impacted the average and ranges of the MAPD. The average MAPD increased from 17.2% for case 1 to 22.6% for case 2, a 5.4% increase. The max MAPD also increased from 42.7% to 56.1%.

The peak of the geomagnetic storm coincided with peak daytime ionization over CONUS during case 2. Case 3 looks at a geomagnetic storm that peaks in the morning over CONUS.

4.5 Case 3 Results

Case 3 is taken from days 95-97 of year 2010. This time frame was chosen as it too occurs during a solar minimum with a geomagnetic storm. The main differences from case 2 are that the timing of the storm is offset from daytime peak ionization, and

the storm is stronger than case 2. This second case was selected to more fully investigate the influence of the timing of a geomagnetic storm on forecast accuracy as well as the extent of the diurnal influence and bias in the model.

4.5.1 CONUS Skill Score

The skill score plot for case 3, Figure 17, shows negative skill scores at night on the first day and during peak daytime ionization on the first day, 22UT day 95, while the Kp values remained elevated (Kp of 4). This is similar to what was observed in both cases 1 and 2 as skill scores decrease and at times become negative either at night when the forecast and reference RMSE were relatively low or during peak daytime ionization during geomagnetic storming.

4.5.2 CONUS RMSE

The RMSE plot for case 3, Figure 18, shows that the errors increase and reach a peak during peak daytime ionization. Peak ionization in case 3 is offset from the peak in the geomagnetic storm, indicated by the max Kp value at ~10UT on day 95. When compared to case 2, the average forecast RMSE for case 3 increases from 2.27 TECU to 2.62 TECU, a 15% increase.

4.5.3 CONUS MPD

The MPD and MAPD plot for case 3, Figure 19, reveals that the greatest MAPD and MPD occur during daytime as it was for case 2. The increased strength in the storm may have influenced the maximum MAPD values. The max MAPD value for case 3 was 88% at 22UT on day 95. The maximum MAPD for case 2 was 56% at 1830UT on day 216, over 30% lower than that for case 3.

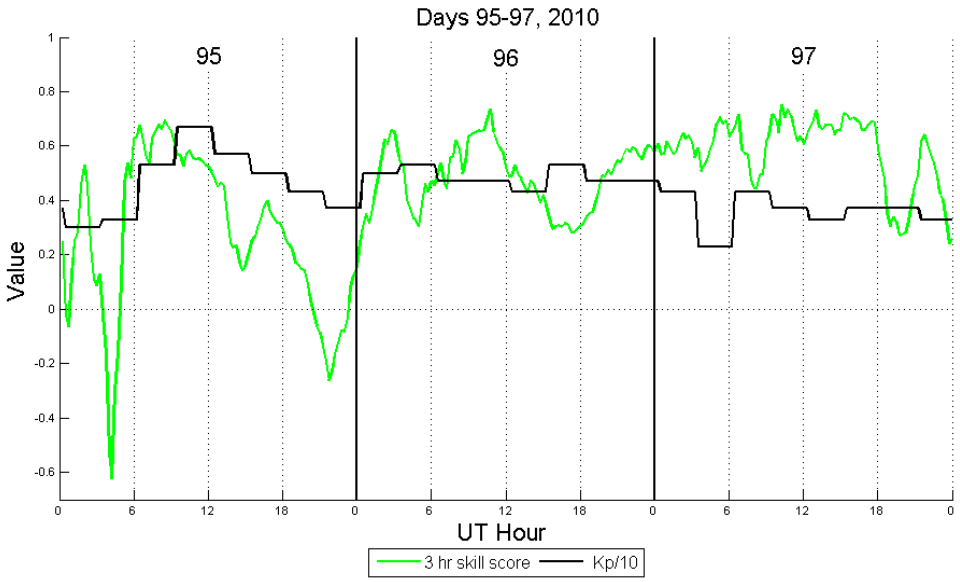

Figure 17. Case 3 skill scores, from days 95-97, 2010.

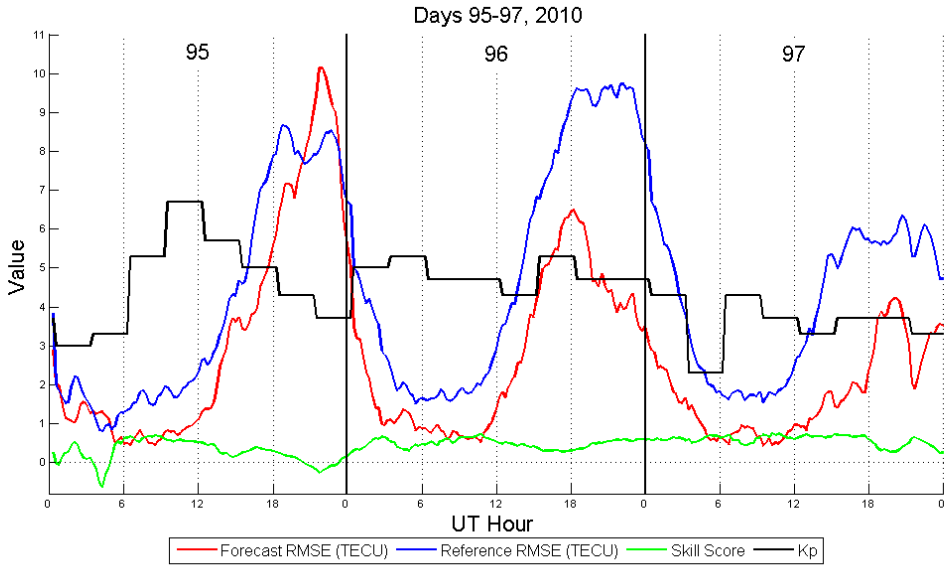

Figure 18. Forecast and reference RMSE and skill scores for case 3, days 95-97, 2010. Note the offset in max storm time (10UT day 95) and peak ionization (22UT day 95). The forecast RMSE (red) is greater than the reference RMSE at 22UT day 95 during storming conditions, similar to case 2.

As with the previous two cases, the MPD also shows a diurnal bias. Whereas the first two cases exhibit the tendency to have negative errors at night, case 3 MPD decrease

at night, but may not become negative, as is seen on day 96 where all MPD values are positive. Further evidence of this is found when taking the average nighttime MPD for case 3 (14.3%) and comparing is to the equivalent results for case 1 (-12.3%) and case 2 (-7.6%) where the latter two are negative. The night timeframe was taken between 0215UT and 0900UT as case 3 is in springtime.

4.6 Case 4 Results

Case 4 encompasses a three day period from day 170-172 in 2001. This time frame was chosen as it corresponds to low geomagnetic activity, similar to case 1, but occurs during a solar maximum period when TEC values are greater when compared to solar minimum. It is also during the summer solstice when the Northern Hemisphere attains maximum solar radiation.

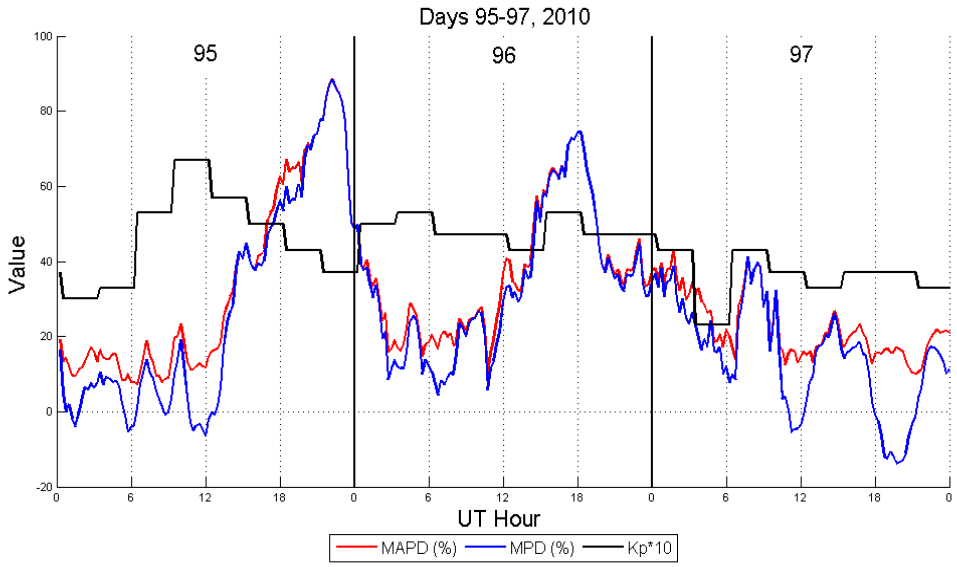

Figure 19. MPD and MAPD for case 3, days 95-97, 2010. Note the peak MAPD of 88% on day 95. Nighttime MDP (0215UT-0900UT) values decrease, but are not necessarily negative as they were fore cases 1 and 2.

4.6.1 CONUS Skill Score

Case 4 skill scores are included in Figure 20. They too show a tendency to increase and decrease throughout the day. The minimum skill score values are offset in case 4 from those in the previous three cases. The decreases are typically seen near 10UT. This time, during the summer solstice, corresponds to sunrise over CONUS which is from 0700UT to 1245UT. Recall that the negative skill scores for the previous three cases occurred near 06UT.

4.6.2 CONUS RMSE

A diurnal pattern is present during solar max, as it was during solar min, with the minimum RMSE attained at sunrise. Because the ratio of the reference RMSE to the forecast RMSE is greater during the daytime than was seen in the previous three cases, the overall skill score for case 4 is the highest of the four cases at 0.51. The average forecast RMSE is greatest in this case at 3.85 TECU compared to 1.43 TECU, 2.26 TECU, 2.61 TECU for cases 1 through 3 respectively.

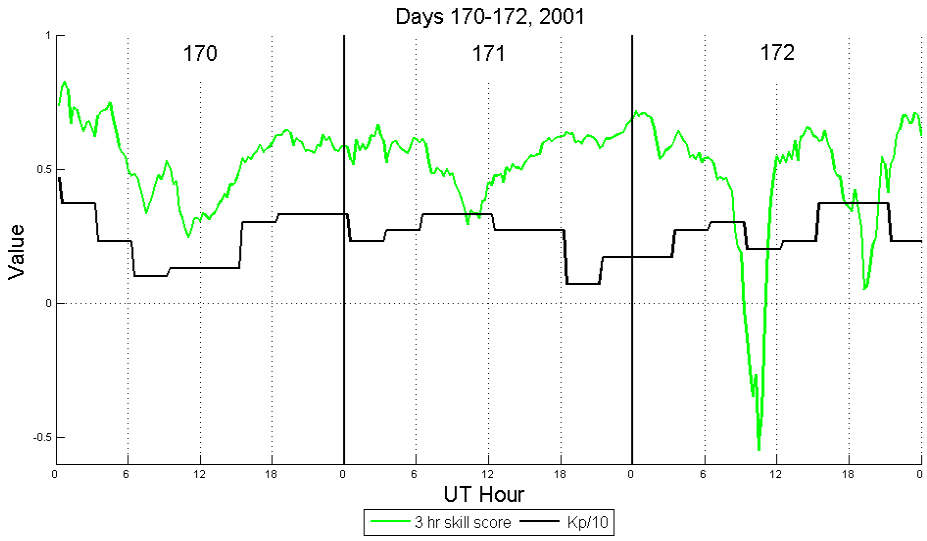

Figure 20. Case 4 skill scores and Kp values for days 170-172, 2001.

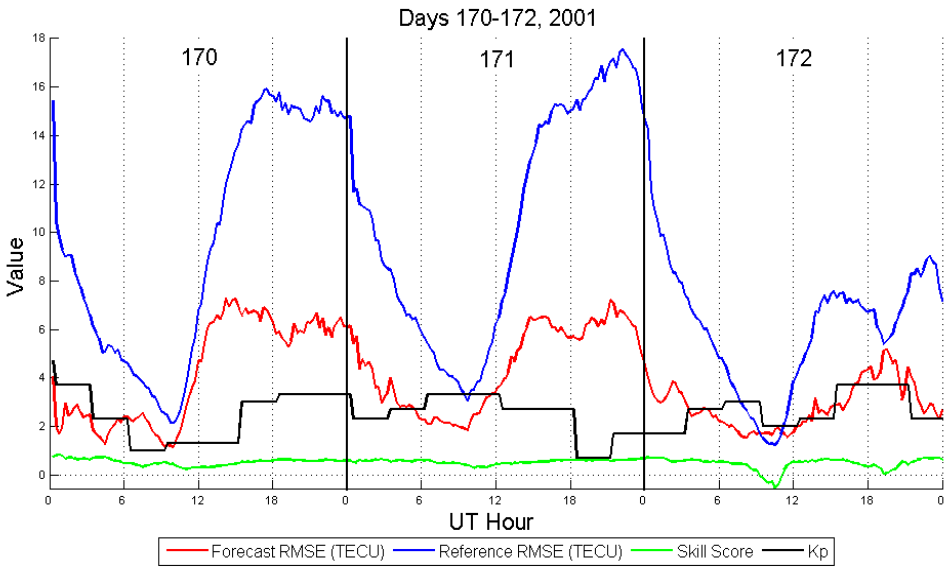

Figure 21. Case 4 forecast and reference RMSE values as well as Kp and skill scores for days 170-172, 2001.

4.6.3 CONUS MPD

The MPD and MAPD fore case 4, Figure 22, show daily peaks for both MPD and MAPD at ~13UT on each of the three days. Daytime and nighttime for case 4 occur between 1245UT and 2230UT and 0400UT and 0700UT respectively. The average nighttime MPD is 3.9% and the daytime MPD is 13.2%. Once again, the MPD is greater during the day than at night.

4.7 Diurnal Comparisons for All Cases

Figure 23, bar charts that show the average daytime and nighttime MPD and RMSE for each case, illustrates the diurnal trend in each of the four cases. The nighttime (blue) bars are less than the daytime (red) bars in every case. Furthermore, in every case, the nighttime values are less than the overall average while the daytime values are greater than the overall values.

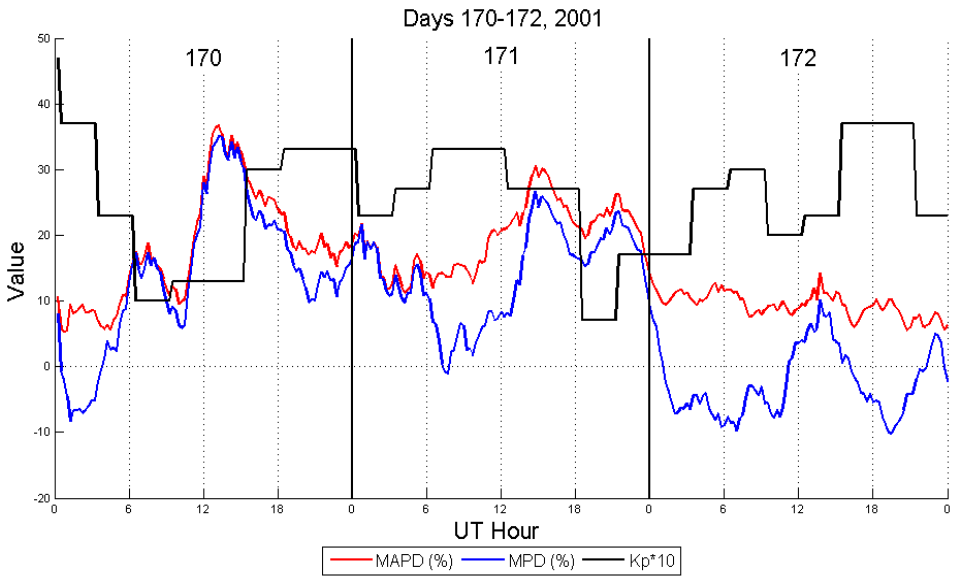

Figure 22. MPD and MAPD for case 4, days 170-172, 2001.

4.8 Forecast Accuracy for Kp Values

There were 1152 forecasts taken from the four cases of the 3-hour forecasts. Average RMSE were plotted by Kp value for this data set and the results are included in Figure 24a. With the exception of Kp values of 5, the average RMSE increases as Kp increases. Results for Kp values of 8 and 9 are absent as the greatest Kp value reached among the four cases was 7. Figure 24b indicates the number of occurrences for each Kp. Numbers of occurrences decreased as Kp increased.

Finally, the average RMSE and Kp correlation was broken up into two categories, quiet and storming, given by Kp values of 0-3 and 4-9 respectively. These are plotted as scatter plots in Figure 25. For such plots, correlation increases as the distribution of the points on the scatter plot becomes less diffuse (more tightly packed around a common trend line). Figure 25a, geomagnetic quiet conditions, is more diffuse and therefore has less correlation than geomagnetic storming conditions, Figure 25b.

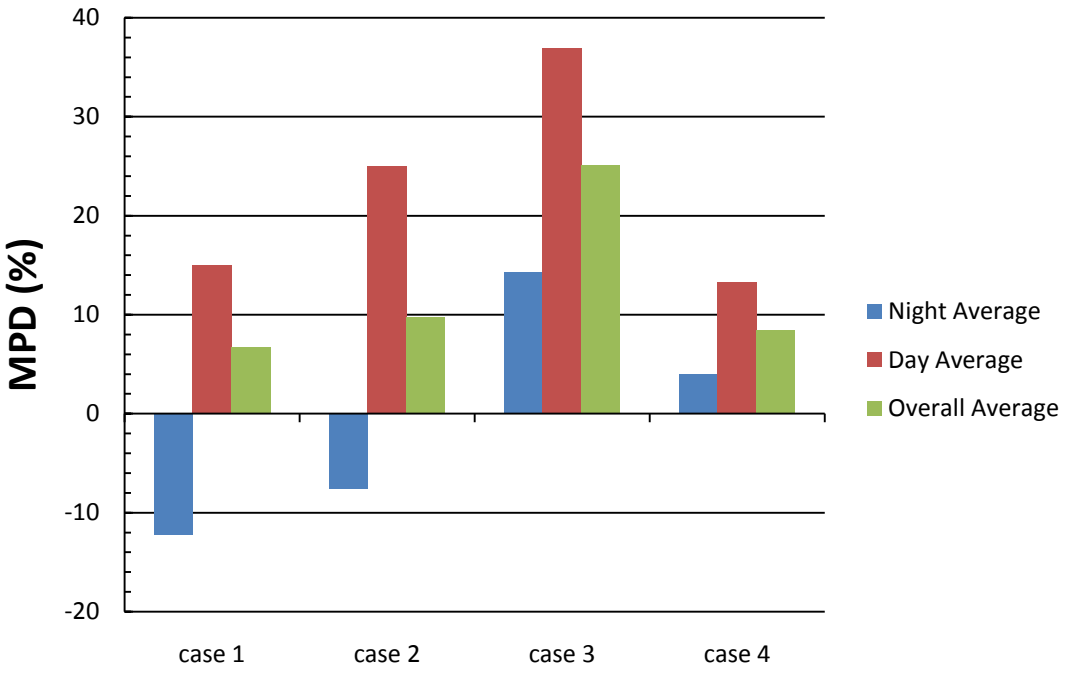

(a) MPD

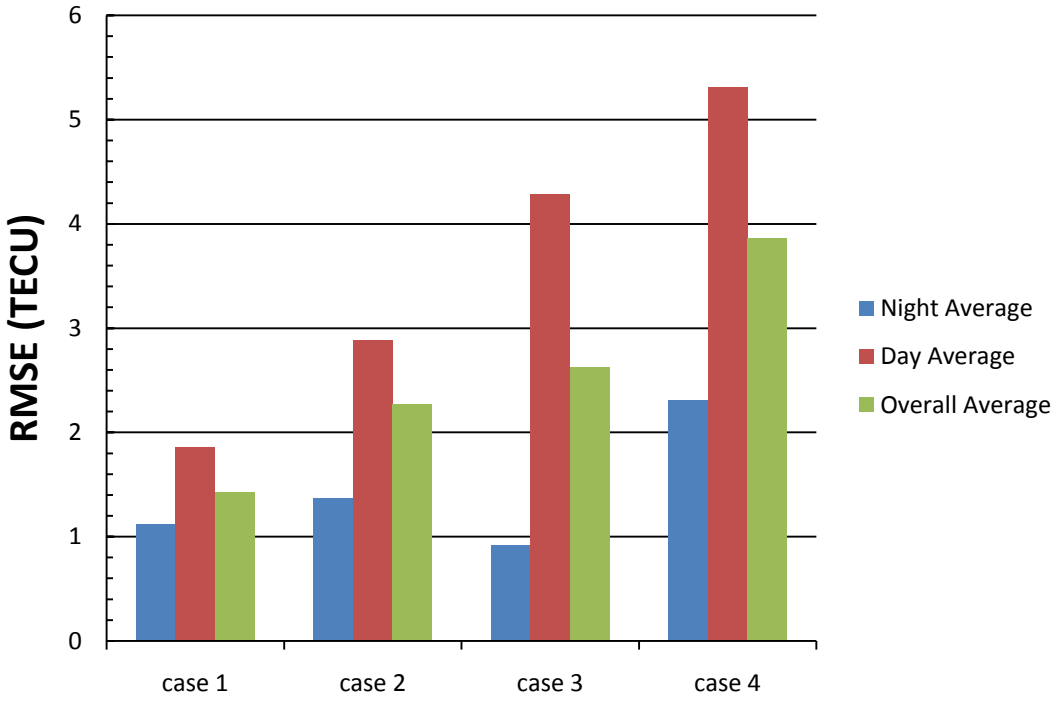

(b) RMSE

Figure 23. Diurnal comparison of (a) MPD and (b) RMSE for all cases. In each case the nighttime values are less than the overall average values and the daytime values are greater than the overall average.

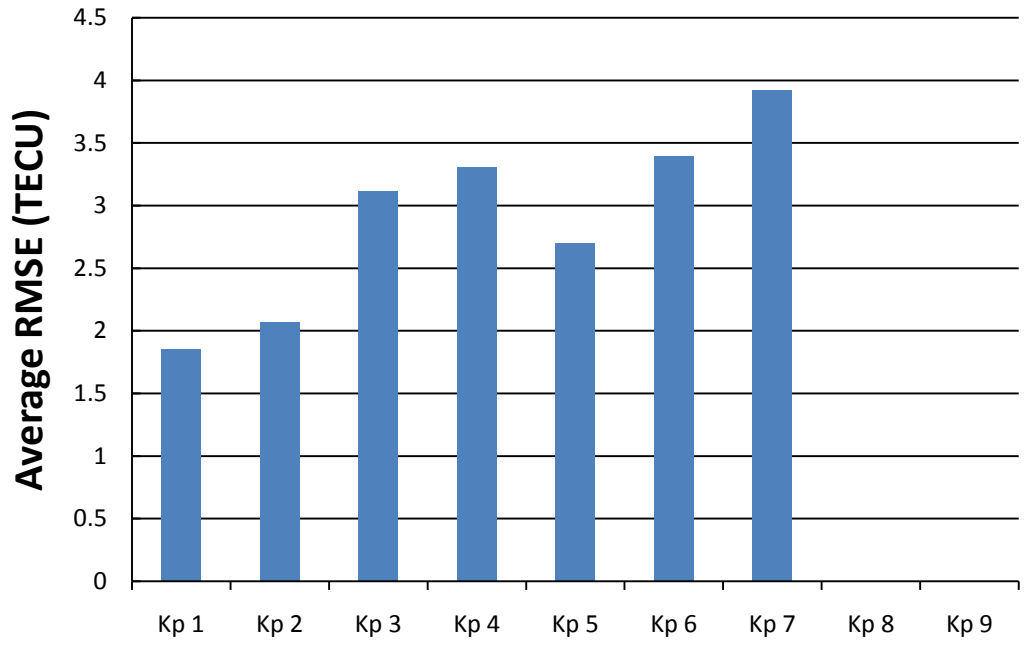

(a) Average RMSE

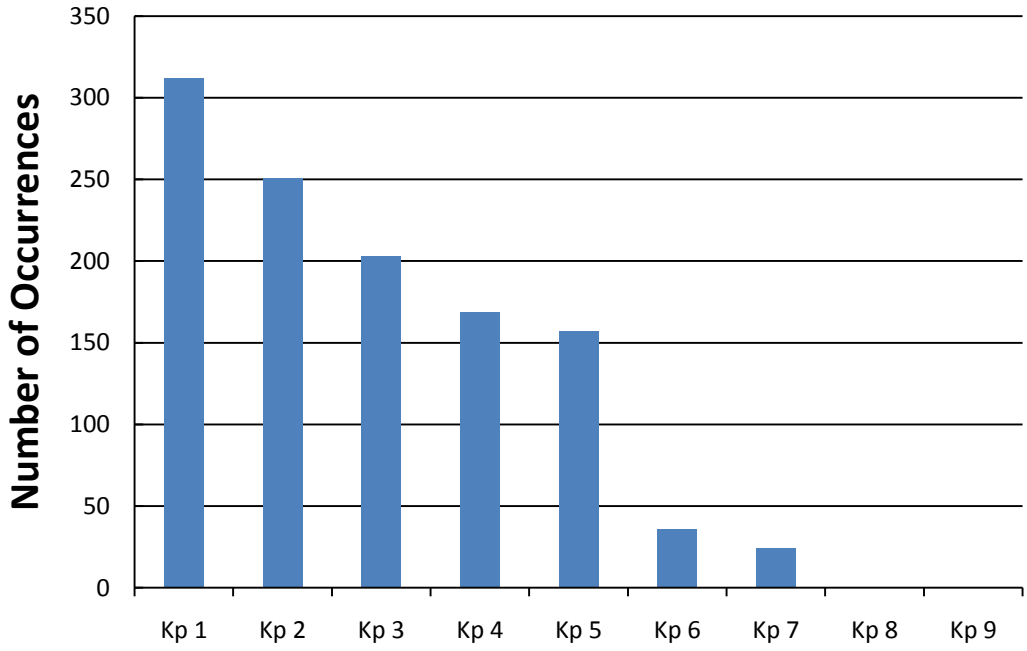

(b) Number of Occurrences

Figure 24. (a) Average RMSE values broken up by Kp value and (b) number of occurrences of each Kp value for the 1152 forecasts over the four cases. Kp values of 7 were the highest observed during the four cases and therefore Kp values of 8 and 9 are not represented.

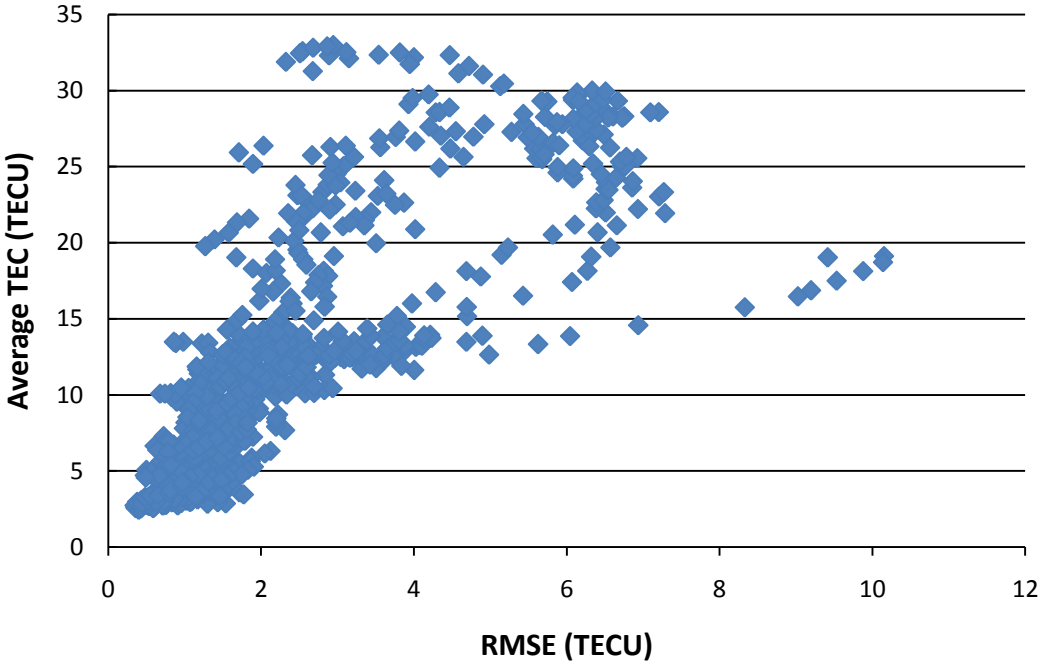

(a) Kp 0-3

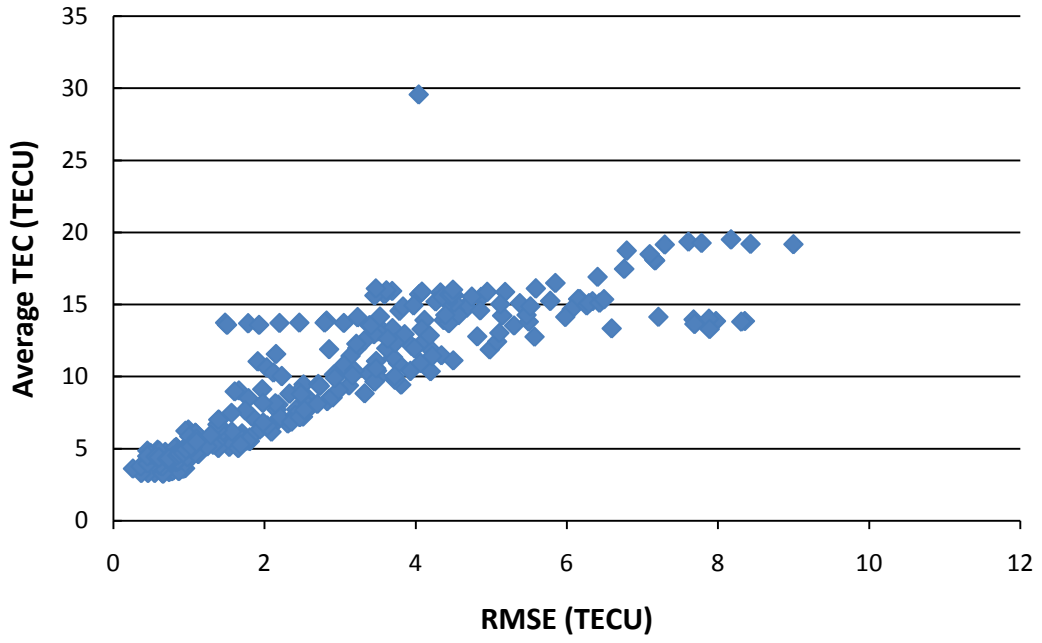

(b) Kp 4-9

Figure 25. Scatter plot of the average TEC values and average RMSE for geomagnetic quiet conditions (a) and storming conditions (b). Geomagnetic storming shows greater correlation than geomagnetic quiet conditions, illustrated by a less diffuse distribution of data points.

V. Conclusions and Recommendations

The two parts of this final chapter include a summary with final conclusions of GAIM-GM accuracy as well as recommendations for future work investigating GAIM-GM model accuracy.

5.1 Conclusions

Knowing the limitations and accuracy of any forecast model is necessary in putting the proper level of confidence into the forecast. GAIM-GM model forecast accuracy was analyzed by comparing forecasts and specifications to a reference background ionosphere derived from IFM output and error covariance matrix of the GAIM-GM Kalman filter. This was done by looking at model accuracy for four cases, corresponding to changes in geomagnetic storming conditions and solar activity variations.

When looking at the percent of positive skill scores, the skill scores, RMSE and MAPD for the forecasts periods averaged over the four cases, the 3-hour forecast accuracy is greatest for all statistical parameters. Moreover, the forecast accuracy degrades as the forecast range increases. The forecast accuracy typically decreases more rapidly from the 3-hour forecast to the 6-hour forecast than from the 12-hour forecast to the 24-hour forecast. The mean forecast skill score, for example, for the 3-hour forecast for all cases is 0.40 and decreases to 0.30 for the 6-hour forecast and finally decreases to 0.25 and 0.23 for the 12 and 24-hour forecasts respectively. This pattern is likewise seen in the RMSE and is perhaps best illustrated in the MAPD where the differences for the 3, 6, 12 and 24-hour forecasts are 21%, 28%, 31% and 32% respectively.

In all four cases, GAIM-GM showed a diurnal forecast trend. The RMSE increased during daytime and decreased at night. Skill scores typically decreased and at times became negative during nighttime as the difference between the forecast and reference RMSE decreased. Finally, with respect to the diurnal pattern, GAIM-GM exhibited a diurnal bias to under forecast at night and over forecast during the day. This was seen in the percent difference plots as the MPD reached minima at night and maxima during the day.

Forecast RMSE typically increased as geomagnetic storming increased. Similarly, forecast RMSE increased as solar activity increased. At times, as the RMSE increased, the skill score increased as well, indicating that the forecast was improving over the reference in representing the ionosphere.

There is a positive correlation between average TEC values and RMSE. This correlation is greater during geomagnetic storming conditions than during quiet geomagnetic conditions.

The GAIM-GM model is able to forecast short term weather phenomena as seen by skill scores greater than zero. Sunrise, sunset and the onset and ending of geomagnetic storms generate low and negative skill scores showing that at times the reference background produces a more reliable forecast than the forecast output itself. Geomagnetic storms and diurnal variation in the ionosphere impact forecast accuracy. Finally, solar minimum accuracy during quiet conditions is greater than solar max accuracy.

5.2 Recommendations for Future Work

Owing to the myriad of variables in the ionosphere and likewise in the configuration of the model, it is impossible for any one study to fully determine model forecast accuracy. The work here presented determined forecast accuracy for GAIM-GM on a global scale with concentration forecast accuracy over CONUS.

To further confirm the efficiency of the Kalman filter and the data assimilation process to obtain accurate forecasts, this analysis should be repeated over other data rich regions such as Europe and Australia. This would give further insight into the diurnal error trends and bias.

This analysis investigated accuracy with respect to TEC. GAIM-GM also forecasts for the ionospherically important height (h_mF_2) and density (N_mF_2) of the F_2 peak in the ionosphere. Hence, the h_mF_2 and N_mF_2 output forecasts accuracy should also be investigated to determine overall accuracy as well as the extent of diurnal error and bias for these parameters.

GAIM-GM is a data assimilation model. The model accuracy was tested in line with how AFWA runs the model. The contributions by various data platforms to forecast accuracy should be investigated. It is possible that other types and combinations of data ingests, as well as data ingest locations could have a significant impact on model forecast accuracy. Testing this may produce output with greater accuracy, determine potential means to reduce or acquire data to keep and improve model accuracy. Work on this topic could impact budgetary issues as access to data costs money. If acceptable accuracy can be achieved with less data, money may be saved.

Bibliography

Delorey, Dennis E., Pruneau, Paul N., Parsons, Carolyn M. (1989), Database Development for the DMSP SSIES Experiment, Space Data Analysis Laboratory, Chestnut Hill, Massachusetts.

Howe, B. M., and K. Runciman (1998), Tomography of the ionosphere: Four-dimensional simulations, *Radio Sci., 33*(1), 109-128, doi: January 2008.

Maybeck, P. S. (1979), *Stochastic models, estimation, and control*, Academic Press, New York.

Ondoh, T., and K. Marubashi (2001), *Science of Space Environment*, Ohmsha, Ltd., Tokyo, Japan.

Scherliess, L., R. W. Schunk, J. J. Sojka, and D. C. Thompson (2004), Development of a physics-based reduced state Kalman filter for the ionosphere, *Radio Sci., 39*(1), RS1S04.

Scherliess, L., R. W. Schunk, J. J. Sojka, D. C. Thompson, and L. Zhu (2006), Utah State University Global Assimilation of Ionospheric Measurements Gauss-Markov Kalman filter model of the ionosphere: Model description and validation, *J.Geophys.Res., 111*(A11), A11315.

Schunk, R. W., and A. Nagy (2009), *Ionospheres: Physics, Plasma Physics, and Chemistry*, Second ed., Cambridge University Press, Cambridge, United Kingdom.

Schunk, R. W., and J. J. Sojka (1995), Development of a Global Ionospheric Forecast Model, Hanscom AFB, Ma.

Schunk, R. W., et al (2004), Global Assimilation of Ionospheric Measurements (GAIM-GM), *Radio Sci., 39*(1), RS1S02.

Sojka, J. J., D. C. Thompson, L. Scherliess, R. W. Schunk, and T. J. Harris (2007), Assessing models for ionospheric weather specifications over Australia during the 2004 Climate and Weather of the Sun-Earth-System (CAWSES) campaign, *J.Geophys.Res., 112*(A9), A09306.

Thompson, D. C., L. Scherliess, J. J. Sojka, and R. W. Schunk (2006), The Utah State University Gauss-Markov Kalman filter of the ionosphere: The effect of slant TEC and electron density profile data on model fidelity, *Journal of Atmospheric and Solar-Terrestrial Physics, 68*, 947-958.

Wilks, D. S. (2006), *Statistical Methods in the Atmospheric Sciences, Volume 100, Second Edition (International Geophysics)*, Second ed., 611 pp., Academic Press, Burlington, Mass.

Zhu, L., R. W. Schunk, G. Jee, L. Scherliess, J. J. Sojka, and D. C. Thompson (2006), Validation study of the Ionosphere Forecast Model using the TOPEX total electron content measurements, *Radio Sci., 41*(5), RS5S11.

Vita

Lieutenant Paul H. Domm graduated from Brighton High School in Rochester, New York in 2000. After serving a 2 year mission for his church, Lt Domm enrolled in The State University of New York College at Brockport and graduated in 2007 with a Bachelor of Science degree in Meteorology. Lt Domm was accepted to Officer Training School at Maxwell AFB, Alabama where he commissioned as a second Lieutenant in the United States Air Force.

His first assignment took him overseas to the 21st Operational Weather Squadron at Sembach AB, Germany. There he fulfilled the roles of Lead Meteorologist and Assistant Flight Commander. After less than two years in Germany, Lt Domm was selected for enrollment into the Space Physics program at the Air Force Institute of Technology at Wright-Patterson AFB, Ohio. Upon graduation, he will serve at the Air Force Weather Agency, Offutt AFB, Nebraska.

REPORT DOCUMENTATION PAGE

Form Approved
OMB No. 074-0188

PLEASE DO NOT RETURN YOUR FORM TO THE ABOVE ADDRESS.

1. REPORT DATE *(DD-MM-YYYY)*	2. REPORT TYPE	3. DATES COVERED *(From – To)*
16-09-2011	Master's Thesis	January 2010 – September 2011

TITLE AND SUBTITLE

Verification of Global Assimilation of Ionospheric Measurements Gauss Markov (GAIM-GM) Model Forecast Accuracy

5a. CONTRACT NUMBER

5b. GRANT NUMBER

5c. PROGRAM ELEMENT NUMBER

6. AUTHOR(S)

Domm, Paul H, 1st Lieutenant, USAF

5d. PROJECT NUMBER

5e. TASK NUMBER

5f. WORK UNIT NUMBER

7. PERFORMING ORGANIZATION NAMES(S) AND ADDRESS(S)

Air Force Institute of Technology
Graduate School of Engineering and Management (AFIT/ENY)
2950 Hobson Way, Building 640
WPAFB OH 45433-8865

8. PERFORMING ORGANIZATION REPORT NUMBER

AFIT/GAP/ENP/11-S01

9. SPONSORING/MONITORING AGENCY NAME(S) AND ADDRESS(ES)

Air Force Weather Agency
101 Nelson Drive
Offutt AFB, NE 68113
DSN 271-0690, COMM 402-294-0690
Email: 2syosdor@offutt.af.mil

10. SPONSOR/MONITOR'S ACRONYM(S)
AFWA

11. SPONSOR/MONITOR'S REPORT NUMBER(S)

12. DISTRIBUTION/AVAILABILITY STATEMENT

APPROVED FOR PUBLIC RELEASE; DISTRIBUTION UNLIMITED.

13. SUPPLEMENTARY NOTES

14. ABSTRACT

GAIM-GM is an operational Kalman filter data assimilation model of the ionosphere that can assimilate data from GPS total electron content (TEC), ionosonde electron density profiles, and satellite based in situ electron densities. The Air Force Weather Agency (AFWA) uses GAIM-GM to specify and forecast the ionosphere. An in depth investigation into the accuracy of these forecasts has not been completed. GAIM-GM output obtained from four cases run from combinations of geomagnetic and solar activity was used to determine GAIM-GM forecast accuracy. Forecast accuracy was determined through the use of a skill score as well as other statistical tools to include root mean square error (RMSE) and percent differences between the forecasts and the observations. It is determined that overall, GAIM-GM forecast output is more representative than the climatological reference 90% of the time indicating that GAIM-GM can therefore forecast short term fluctuations in the ionosphere. The RMSE increases during daytime, geomagnetic storming and during solar maximum. Skill scores decrease at night and GAIM-GM shows an overall diurnal bias to under forecast at night and over forecast during the day.

15. SUBJECT TERMS

Ionosphere, Ionospheric Forecast Model, Global Assimilation of Ionospheric Measurements Gauss Markov Kalman Filter (GAIM-GMKF), Space Weather

16. SECURITY CLASSIFICATION OF:			17. LIMITATION OF ABSTRACT	18. NUMBER OF PAGES	19a. NAME OF RESPONSIBLE PERSON
a. REPORT	b. ABSTRACT	c. THIS PAGE			Robb M. Randall, Lt Col, USAF ADVISOR
U	U	U	UU	68	19b. TELEPHONE NUMBER *(Include area code)* (402) 294-9544, (robb.randall@us.af.mil)

Standard Form 298 (Rev. 8-98)
Prescribed by ANSI Std. Z39-18